



Depositional facies, architecture and environments of the Sihwa Formation (Lower Cretaceous), mid-west Korea with special reference to dinosaur eggs

S.B. Kim^{a,*}, Y.-G. Kim^b, H.R. Jo^c, K.S. Jeong^d, S.K. Chough^{b,*}

^a Korea Polar Research Institute, Korea Ocean Research and Development Institute, Ansan 426-744, Republic of Korea

^b School of Earth and Environmental Sciences, Seoul National University, Seoul 151-747, Republic of Korea

^c Department of Earth and Environmental Sciences, Andong National University, Andong 760-749, Republic of Korea

^d Marine Geoenvironment and Resources Research Division, Korea Ocean Research and Development Institute, Ansan 425-600, Republic of Korea

ARTICLE INFO

Article history:

Received 23 May 2007

Accepted in revised form 15 May 2008

Available online 13 June 2008

Keywords:

Alluvial fan

Ephemeral braided stream

Depositional facies and architecture

Dinosaur egg and nest

Sihwa Formation

Cretaceous

ABSTRACT

This paper presents detailed facies and architectural analyses and palaeoenvironmental reconstruction of the Sihwa Formation (Lower Cretaceous), mid-west Korea, which comprises an about 3-km-thick non-marine succession containing abundant dinosaur eggshells. Based on constituent facies, bedset geometry, stacking pattern, and bounding surface characteristics, the entire succession can be classified into three architectural elements. Element I occurs along the basin margin and shows a monotonous stacking of tabular or crudely stratified conglomeratic units. It represents alluvial-fan deposits of debris-flow-dominated fan and sheetflood-dominated fan. Element II is characterized by multi-storey, sheet or upward-widening, conglomeratic channel-fills whose maximum thickness exceeds 1.5 m. Each channel-fill unit is encased within red-brown silty sandstones of Element III with sharp erosional bases but diffuse gradational upper boundaries. It consists generally of (1) cut-and-fill deposit (trough cross-stratified or openwork conglomerate) in the lower part and (2) composite low-relief bar deposit (lenticular conglomerate and stratified gravelly sandstone) in the upper part. Shallowness of each cut-and-fill unit, absence of fining-upward lateral accretion package and the predominance of simple-bar deposit collectively suggest deposition from ephemeral braided streams. Element III typically shows a fining-upward stacking of (1) single- or multi-storey small-scale (<1.5 m thick) channel fills with limited lateral extent of less than 15 m, (2) poorly sorted, graded and diffusely bounded silty conglomerates or gravelly siltstones with discontinuous gravel sheets and pockets and (3) homogeneous or graded, red-brown fine-grained deposits with calcretes and burrows in ascending order. Element III is interpreted as channel-margin to floodplain, including crevasse channel fill, crevasse splay and floodplain fines.

The entire sequence of the Sihwa Formation can be divided into the alluvial-fan and terminal-fan successions. The alluvial-fan succession displays a progradational stacking pattern and indicates a low rate of basin subsidence in the initial phase of rifting. The upper terminal-fan succession consists of proximal braided stream and distal floodplain deposits in the western and central parts of the basin and is characterized by an axial dispersal pattern and an aggradational stacking. It suggests rapid subsidence of the basin floor during the main phase of rifting. The asymmetrical cross-basin distribution of each architectural element reflects a half-graben structure of the basin with steep-gradient fault-bounded eastern margin (footwall block) and gently sloped, flexural western margin (hangingwall block). The predominance of ephemeral braided-stream deposits along with red-brown fine-grained floodplain deposits with common calcretes indicates arid to semi-arid palaeoclimates.

Approximately 140 dinosaur eggs (Faveoololithidae and Dendroolithidae) were identified mainly from the (gravelly) siltstones and small-scale channel fills of Element III deposits and partly from the cut-and-fill conglomerates of Element II deposits. The eggs commonly retain their original oval shape but are invariably breached and stuffed with the substrate of gravels and silt. They are either isolated or

* Corresponding authors. Domestic E&P Department, Korea National Oil Corporation, Anyang 431-711, Republic of Korea (S.B. Kim).

E-mail address: sedlab@snu.ac.kr (S.K. Chough).

clustered, forming a circular concentration in plan view. The abundant yield of eggs, more than 20 eggs in 5 separate nests from a single depositional unit, suggests a dense population of the parental dinosaurs. The repetitive occurrence in many stratigraphic horizons reflects site preference as a nesting habitat of the near-channel or abandoned channel areas.

© 2008 Elsevier Ltd. All rights reserved.

1. Introduction

The Cretaceous deposits of the Korean peninsula have recently been recognized as fossiliferous strata yielding abundant dinosaur footprints, eggs and bones (Lee et al., 2001; Huh et al., 2003) (Fig. 1). Detailed bed-by-bed facies analysis and basin-wide architectural analysis of the fossil-bearing deposits are, however, rarely made with regard to fossil preservation and palaeoecological interpretations (Paik et al., 2001a, 2001b, 2004). Poor knowledge on the depositional

processes and environments not only hampers proper palaeoecological understanding but also may lead to the erroneous interpretations from reworked fossils.

The Sihwa Basin, mid-west Korea (Figs. 1 and 2) comprises a fossiliferous non-marine succession of the Lower Cretaceous (Sihwa Formation) that has yielded more than 140 dinosaur eggs of the families Faveoolithidae and Dendroolithidae. These eggs commonly occur as circular clusters with 3–12 eggs in 1–2 layers and thus are interpreted as nests (Lee et al., 2000). The eggshells

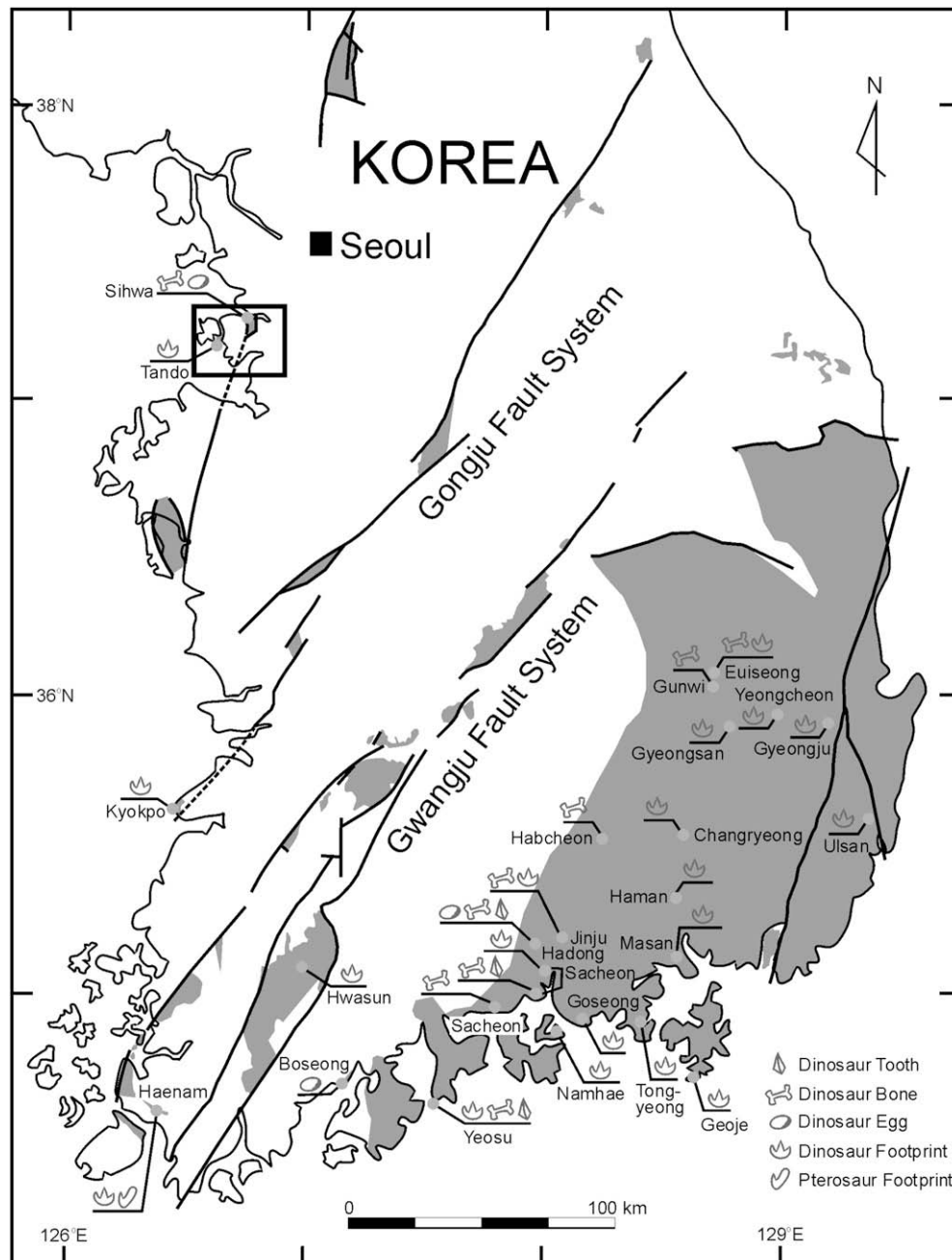


Fig. 1. Distribution of Cretaceous sedimentary basins (shaded areas) and fault patterns in the Korean peninsula (modified after Chough et al., 2000). Locations of dinosaur footprints, eggshells, bones and teeth, and pterosaur footprints are also depicted (compiled after Lee et al., 2001; Huh et al., 2003). Rectangle represents the study area.

are, however, characteristically breached or holed and completely stuffed with substrate sediment (gravels and silt), whereas the original oval shape is largely retained. This indicates the possibility of displacements or disturbance of eggs and requires careful sedimentologic examinations for their preservation whether being in intact clutches or scattered out of nests.

For this study we have conducted detailed facies and architectural analyses of the Sihwa Formation in order to reconstruct palaeoenvironments and the distribution of depositional systems on a basin-wide scale. Particular attention is paid to the characteristics of the deposits containing dinosaur eggs in order to clarify their *in situ* burial and the dinosaur's nesting habitus. Criteria for distinguishing displaced eggs from intact preserved nests are put forward. This study indicates the importance of sedimentological analysis as a firm ground for the comprehension of the taphonomic processes as well as for advanced palaeoecological interpretations, such as site fidelity or preferential habitat for a certain environment.

2. Geological setting

In the southern part of the Korean peninsula, a number of non-marine basins formed along a series of NE–SW-trending left-lateral

strike-slip fault systems during the Cretaceous (Chun and Chough, 1992; Chough et al., 2000) (Fig. 1). The fault systems resulted from intracontinental transcurrent tectonics caused by oblique northward subduction of the Izanagi plate below the Eurasia plate during the Jurassic to Early Cretaceous (Kim et al., 1997; Chough et al., 2000). The associated rhomboidal basins were filled with alluvial to lacustrine deposits during the Early and Late Cretaceous (Lee, 1999; Chough et al., 2000).

The Sihwa Basin is located in mid-west Korea (Fig. 1). It is bounded by N–S trending faults in the eastern and western margins (Park and Kim, 1972; Park, 2000; Park et al., 2000; Hwasung City, 2005) (Figs. 2 and 3a). Transtensional opening of the basin due to dextral strike-slips on the eastern border fault has been suggested, based on the fault bend geometry and the development of NW–SE-trending intrabasinal folds (Hwasung City, 2005). The counter-clockwise rotation or drags of the sedimentary strata along the eastern border fault also supports the dextral slips of the eastern footwall block relative to the basin floor. It is interesting to note that the axis of intrabasinal folds forms an acute (ca. 30°) junction to the border fault (Fig. 3a), which suggests a deformation in an E–W-direction transpressional regime (Hwasung City, 2005; cf. Sander and Marchini, 1984). Due to the transpression, basin growth was most likely conducted mainly in N–S direction (i.e. northward

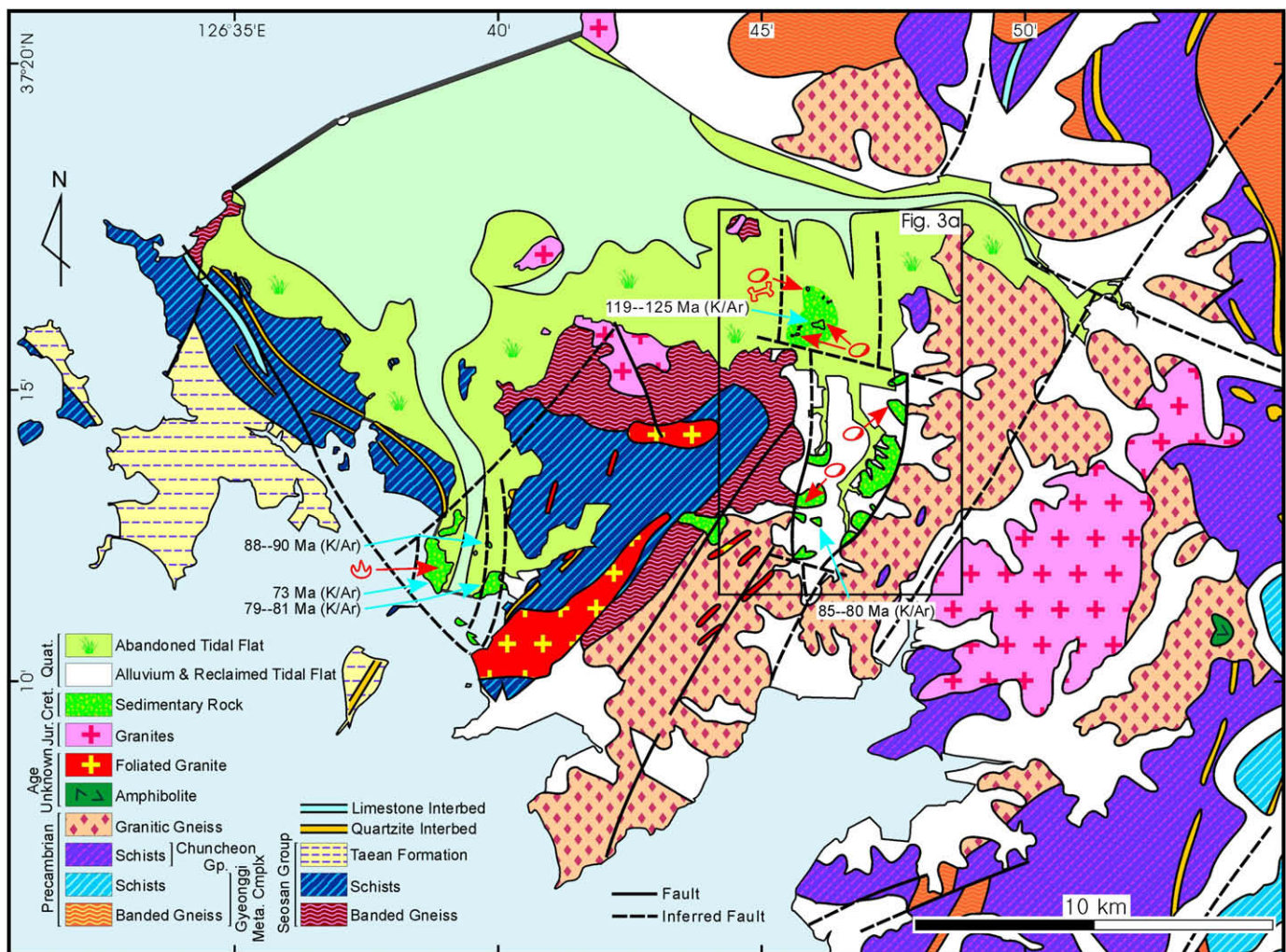


Fig. 2. Regional geologic map of study area (modified after Park and Kim, 1972; Lee et al., 1999a, 1999b; Park, 2000). Cretaceous sedimentary rocks are unconformably underlain by the basement of Precambrian metamorphic and Mesozoic plutonic rocks, deposited mainly in the fault-bounded basins (Sihwa and Tando basins). Locations of dinosaur remains and dated volcanic samples are also depicted. Age data are collected from this study (the northern part of Sihwa Basin, Park (2000); the southern part of the Sihwa Basin and the eastern part of Tando Basin), and Choe et al. (2001; the western part of the Tando Basin).

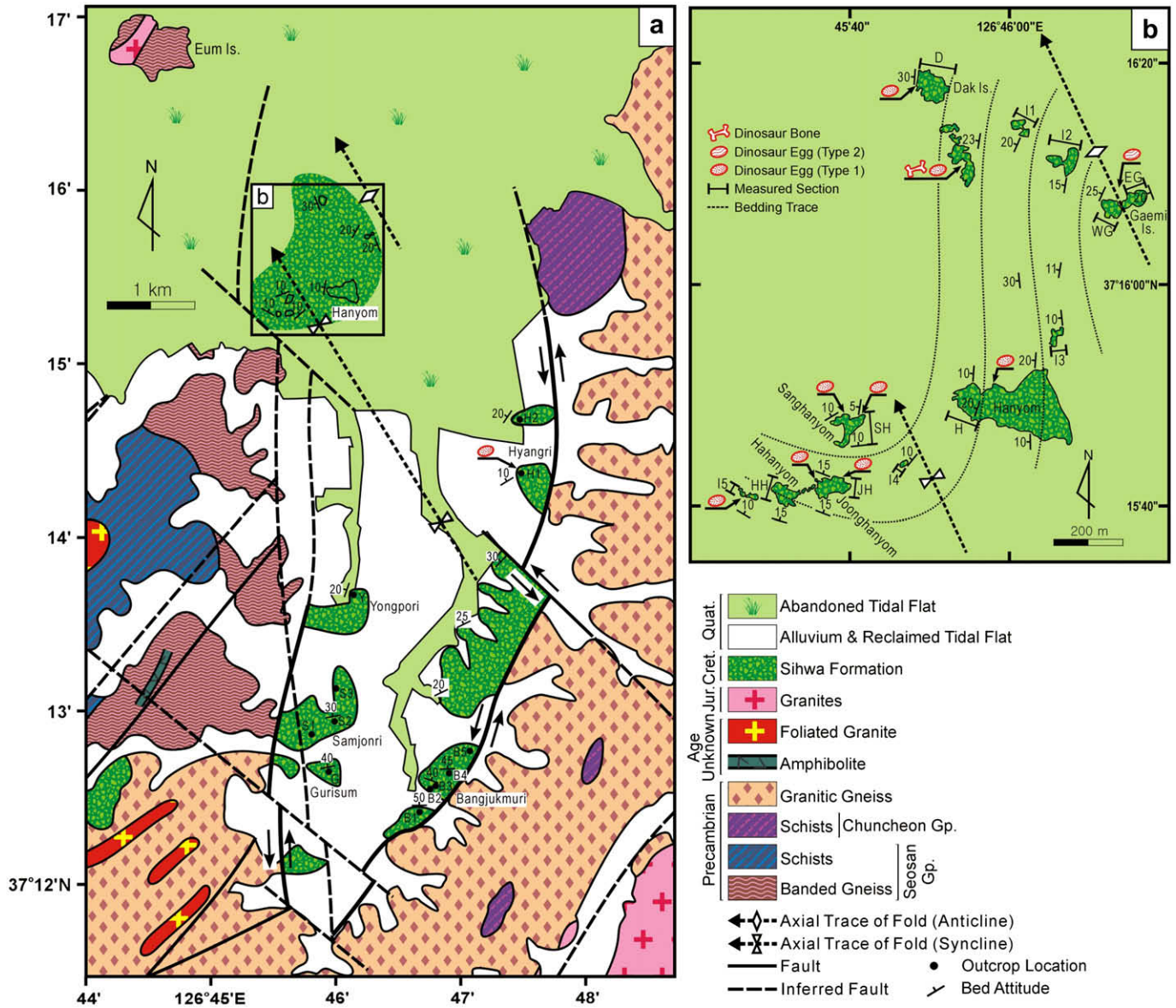


Fig. 3. (a) Geologic map of the Sihwa Basin (modified after Park and Kim, 1972; Park, 2000; Hwasung City, 2005). Locations of measured sections and dinosaur remains are denoted. (b) Detailed map of the northwestern part (Hanyom area) of the basin (modified after Hwasung City, 2005).

propagation) as indicated by the progressive younging of the basin-fill sediment in the northward direction. The northward basin extension was presumably accommodated by the formation of a series of southward-dipping NE–SW normal faults and thereby segmentation of basin floor into a series of northward-tilted fault blocks (Hwasung City, 2005).

The NW–SE-trending fault crossing the medial part of the Sihwa Basin cutting the N–S-trending basin-bounding faults (Fig. 3a) may have resulted from the synthetic (sinistral) R' shear during the basin inversion, although its apparent left-lateral sense of movement is incompatible with the Riedel shear model. Such a reversal of fault movement can only be accounted for by the sinistral reactivation of the boarder fault. Such a reversal of fault movement or basin inversion is a common feature in the cognate Cretaceous basins in the Korean peninsula (e.g., Lambiase and Bosworth, 1995).

The Sihwa Basin rests on the basement of Precambrian gneiss and schist and Mesozoic granite, and contains a Cretaceous sedimentary succession (Sihwa Formation). The Sihwa Formation comprises stratigraphically an about 3-km-thick alluvial deposits of conglomerate, gravelly sandstone, sandstone and red–brown

siltstone. Clasts are composed mainly of granitic gneiss, banded gneiss, green or blue schist and quartzite with subordinate amounts of limestone, granite and volcanic rocks. K–Ar whole-rock age of a tuff clast in a conglomerate bed is 85–80 Ma (Park, 2000; Fig. 2), which probably indicates a reset age affected by argon loss during postdepositional hydrothermal alteration in the basin margin. Using the same method, alternative ages of 119.8 ± 2.3 Ma (basalt dyke), 118.6 ± 2.3 Ma (ignimbrite clast) and 125.5 ± 2.4 Ma (basalt clast) are obtained in the central part of the basin (Fig. 2), which are more comparable with the correlated age of the dinosaur eggs of the Early Cretaceous (Lee et al., 2000). The newly obtained ages of reworked volcanic clasts are believed to represent the depositional ages, because volcanic activities were commonly associated with the basin initiation (Lee, 1999; Chough et al., 2000).

More than 140 dinosaur eggs have been identified from the Sihwa Formation (Hwasung City, 2005). Detailed taxonomic analysis indicates that the eggs can be classified into two types (Lee et al., 2000). Type 1 eggs are characterized by a thin shell (0.85–1.23 mm) and circular pore canals, whereas type 2 eggs consist of a thick shell (3.4–5.0 mm) possessing longitudinal

furrows on the outer shell surface. The former can be referred to *Youngoolithus xianguanensis* (Zhao, 1979) of Faveoololithidae (Zhao and Ding, 1976) and the latter to Dendroolithidae (Zhao and Li, 1988). The eggs commonly occur as clustered horizons of 1–2 layers and reveal circular concentration (ca. 50–60 cm in diameter) of 3–9 eggs in plan view, which appear to represent intact preserved clutch-type nests (Lee et al., 2000).

3. Sedimentary facies and architectural analyses

Based on lithology (grain size), bed geometry and internal structures, eleven sedimentary facies are identified in the Sihwa Formation. Table 1 details the characteristics and inferred depositional processes for each facies. The deposits can be grouped into seven facies associations (or subelements) and further into three architectural elements (Table 2), based on constituent facies, bedset geometry, stacking pattern, and bounding surface characteristics. Fig. 4 summarizes parts of sedimentary columns in the northern Sihwa Basin as well as horizons of egg occurrence, burrow, and calcareous nodules. Each element or facies association (FA) records deposition in a distinct depositional environment: (1) alluvial fan (Element I), either debris-flow-dominated fan (FA IA) or sheetflood-dominated fan (FA IB), (2) ephemeral braided stream (Element II) comprising either cut-and-fills (FA IIA) and/or low-relief bars (FA IIB) and (3) channel margin to floodplain (Element III) constituted by crevasse channels (FA IIIA), crevasse splays (FA IIIB) and floodplain fines (FA IIIC) (Table 2).

3.1. Element I: alluvial fan

Element I is represented by monotonous stacking of tabular or crudely stratified conglomeratic units (facies Gt or GSs) with occasional intervening fine-grained deposits (Figs. 5 and 6). Each depositional unit generally ranges in thickness from 30 to 100 cm. Clasts are mostly pebble to cobble grade with subordinate amounts of boulders (up to 70 cm long) and are generally angular to sub-angular. Element I deposits occur mainly along the eastern basin margin and partly extend to the basin center. It is divided into two types, according to the dominant constituent facies: FA IA dominated by tabular conglomerates (facies Gt) and FA IB largely by crudely stratified conglomerate/sandstone couplets (facies GSs).

3.1.1. FA IA: debris-flow-dominated fan

Description: FA IA occurs mainly along the eastern basin margin in the southern basin sector (Sections B1–B5, G and H2) and partly extends to the basin center, where it sharply overlies FA IIIA deposit. It consists entirely of tabular conglomerates (facies Gt) with thin intercalation of graded sandstone or red-brown siltstone (Fig. 5). Each conglomerate unit ranges in thickness from 25 cm to more than 1.5 m and is laterally persistent over the entire outcrop (>10 m in lateral extent). Each bed is sharply based with planar surface but the upper boundary is usually undulatory or irregular with common protruding clasts. Clasts are predominantly angular and range in size mostly from pebble to cobble grade. They are inversely or inverse-to-normally graded and are either matrix- or clast-supported, particularly in the clast-rich upper part. Large boulder-size clasts generally occur floating in the middle part of the bed or protruding along the upper boundaries. Elongate clasts commonly reveal an orientation parallel to that of the bedding surface. Matrix material comprises poorly sorted, coarse-grained sandstone and siltstone locally along the upper boundaries. The sandstone beds are generally planar, whereas the siltstones are discontinuous and form lenses or pockets. Both are less than 10 cm thick and commonly contain pebble clasts (Fig. 5c).

Some beds of tabular conglomerate include laterally overlapping wedges (Fig. 5a, b). The wedges are inversely graded and

become thinner and tangentially pinch out toward the downdip margins where largest clasts are concentrated. Superposition of the finer-grained rear part of the overlying wedge on the coarse-grained front of the underlying one produces a “false” normal grading (Fig. 5a, b). It is also notable that other conglomerate beds show tightly interlocked, locally openwork gravel concentrations along the planar-topped upper boundaries (Fig. 5d). In this case, there occurs an abrupt increase in clast size and abundance accompanied with a pronounced decrease in grain size of the matrix material across the gravel horizon.

Interpretation: The tabular-bedded nature, common floating or protruding oversized clasts, preferred flat-lying clast orientation and the undulatory upper surfaces of the conglomerate units (facies Gt) indicate deposition from laminar plastic flows. The common inverse grading of gravel clasts with framework support in sandstone matrix specifically suggests cohesionless debris flow in which inertial grain interaction is dominant (Nemec and Steel, 1984; Kim et al., 1995; Sohn et al., 1999). Although similar sand-matrix gravelly deposits have been interpreted as hyperconcentrated flows (e.g., Mulder and Alexander, 2001), the present deposits lack reliable evidence for flow turbulence, such as scours, traction structures and normal grading, and thus are regarded as resulting from laminar flows.

The good lateral continuity of each sedimentation unit and the lack of channel incision suggest deposition from unconfined flows. The relative thinness of the depositional unit, compared to the constituent clast size, however, indicates low flow mobility. The deposits are envisaged as debris lobes at the termini of self-confined or leveed debris flows (Sharp and Nobles, 1953; Wells and Harvey, 1987; Kim and Lowe, 2004). Pulsatory surges in the feeding debris flows are further postulated based on the overlapping wedge-like subunits in a single sedimentation unit. Each wedge may represent individual surges that are self-organized into the coarse-grained head and trailing finer-grained tail. A tangentially pinching-out snout is a characteristic depositional feature of water-saturated debris flows (Major, 1997). The intervening sandstone and siltstone intercalations probably resulted from the trailing tails that comprised some bedload pebbles. The overlapping of wedge-shaped subunits (Fig. 5a, b) may have formed when a succeeding surge took up the deposit of a preceding one. Similar overlapping wedges were also observed from submarine debris-flow deposits, showing a reverse downdip organization, i.e., younger surge stacked up behind the older surge (Sohn et al., 1997). The occasional tightly packed or armoured gravel concentrations along the upper bedding surface (Fig. 5d) may have resulted from reworking and winnowing by the following watery flows (Major, 1997; Blair, 1999a).

The basin-marginal accumulation of bouldery debris-flow deposits is reminiscent of alluvial-fan environment (Nilsen, 1982). Because of the limit in available outcrops, radial dispersal pattern or facies changes cannot be discerned; nevertheless, the above inferred rheodynamics of the debris flows is strongly indicative of a steep-gradient alluvial setting rather than low-gradient fluvial plains. The predominance of angular clasts also supports this inference in that minimum abrasion occurred during the course of basinward transport from the hinterland drainage areas. Development of surging debris flows has been widely observed in alluvial fans and can be accounted for by the generation of “roll waves” due to the steep gradient (Davies, 1986, 1990) or fluctuating bedload discharge at the valley mouth.

3.1.2. FA IB: sheetflood-dominated fan

Description: FA IB occurs in the northern basin sector (Sections WG and I3), interfingering with FA IIIA deposit. It comprises a ca. 30-m-thick succession of crudely stratified conglomerate/sandstone couplets (facies GSs) with minor amounts of hollow filling, openwork lenticular conglomerate (facies Glo) and red-brown siltstone

Table 1

Description and interpretation of sedimentary facies in the Sihwa Formation

Facies	Description	Interpretation
Tabular conglomerate (facies Gt)	0.25–1 m thick; laterally continuous (>10 m); planar sharp lower boundary and slightly irregular upper boundary with common protruding clasts; inversely or inverse-to-normally graded; matrix- or clast-supported; common parallel oriented clasts; pebble to cobble-size clast common with occasional oversized boulders; poorly sorted, coarse-grained sandstone matrix; common lensoidal or pocket-shaped siltstone intercalations with pebbles; internal, laterally overlapping wedges; occasional armored gravel concentrations along upper boundary	Cohesionless debris flow (Nemec and Steel, 1984; Kim et al., 1995; Sohn et al., 1999)
Gravel sheet (facies Gs)	A few clast to decimetres thick, laterally continuous (> 10 m); tabular or wedged with flat or shallowly concave-up base and planar or slightly convex-up upper boundary; densely packed pebble–cobble clasts with a paucity of sandstone matrix in the central part; less densely packed, pebble-dominant wedged margins with greater amounts of matrix material of silty sandstone; laterally transitional into discontinuous pebble–cobble trains; stacked repeatedly or interlayered with facies Fh units	Bedload deposition as gravel sheets or splays by high-magnitude flood flows (Stear, 1983; Rhee and Chough, 1993a,b; Bristow et al., 1999)
Gravel pocket (facies Gp)	One to a few clast thick; less than a few metres wide; lenticular or pocket-shaped, clast-supported granule–pebble deposit, or loosely packed, discontinuous pebble train; slightly contorted in places; encased within facies Fh units	Bedload deposition as gravel streams or lineaments by weak distal flood flows (Jo, 2003)
Open-work lenticular conglomerate (facies Glo)	Resting above a scour hollow (decimetres to metres in width and decimetres in depth), completely filling-up or forming a thin basal veneer, one to several-clast-thick; mainly cobble-grade clasts with occasional pebbles and boulders; tightly interlocked with open framework or small amounts of fine- to coarse-grained interstitial sandstone	Channel lag or gully-fill deposit (Nemec and Postma, 1993; Blair, 1999b, 2000)
Clast-supported lenticular conglomerate (facies Glc)	10–50 cm thick; lenticular, a few metres wide (max. 20 m), either planar-convex, concave-planar or biconvex; sharp lower boundary and relatively indistinct upper boundary; cobble–boulder core and pebbly fringes; laterally or vertically transitional into facies GySix or GySh units Core: tightly interlocked; disorganized; matrix deficient or infiltrated silty sandstone Fringes: thinner than core; common clast imbrication; normally or more commonly inversely graded; coarse-grained sandstone matrix	Low-relief longitudinal gravel-bar (Boothroyd and Ashley, 1975; Miall, 1985; Karpeta, 1993; Jo et al., 1997)
Trough cross-stratified conglomerate to gravelly sandstone (facies Gtx)	Resting above a scour hollow (decimetres to metres in width and decimetres in depth), completely filling-up or above basal veneer of facies Glo; alternations of tightly packed, pebble-cobble conglomerate (one- to several-clast-thick) layer and massive or trough cross-stratified coarse sandstone (up to 15 cm thick) layer; each layer gently dipping (<15°), generally conforming the topography of the basal scour hollow; single sets predominant, cosets rare; each set commonly fining- and thinning-upward 30–80 cm thick; laterally continuous (>10 m); generally abruptly normally graded with lower conglomerate and upper sandstone divisions	Infills of minor channels (Miall, 1977, 1985; Khadkikar, 1999; Jo and Chough, 2001)
Crudely stratified conglomerate/sandstone couplets (facies GSs)	Conglomerate division: laterally discontinuous a few metres apart; a-few-clast thick; sharp planar, locally scooped erosional base; tightly interlocked clasts with a paucity of sandstone matrix Sandstone division: usually thicker than lower division, moderately sorted, coarse-grained sandstone, massive or normally graded with well-laminated tops	Sheetflood (Blair, 1987, 1999b, 2000)
Graded conglomerate/siltstone couplet or conglomerate/sandstone/siltstone triplet (facies GZg)	Decimetres to >1 m thick; laterally continuous a few decimetres; tabular bedded; diffusely or indistinctly bounded; distribution-type graded with pebble–cobble silty conglomerate at the base and normally graded siltstone at top, intervened or not by an interval of silty sandstone; stacked repeatedly showing an overall fining- and thinning-upward trend Conglomerate division: loosely packed clasts with matrix- to clast-supported fabric; partly, diffusely and discontinuously stratified with local clusters; deformed in places; common clast imbrication; sandy siltstone matrix Sandstone division: ungraded or graded; unstratified; moderately sorted; dominantly coarse-grained; silty interstitial material Siltstone division: poorly sorted, distribution-type or coarse-tail graded with sandy base; non-fissile; red–brown in colour	Successive bedload and suspension sedimentation from unconfined, rapidly waning flood flows
Horizontally stratified gravelly sandstone (facies GySh)	A few decimetres thick; a few metres to decametres wide; alternating layers (1–10 cm thick) of pebbly coarse-grained sandstone and medium- to fine-grained sandstone; each layer (sub-)parallel, slightly undulatory or low-amplitude wavy; common lateral layer splitting or convergence; individual layers either ungraded, normally or inversely graded or locally interstratified; pebbles either flat-lying or imbricated; occasional oversized cobbles and boulders; laterally juxtaposed with or transitionally overlying facies Glc or GySh units	Low-relief or plane-bedded bar (Allen, 1983) or upper-plane-bedded shoals or interbar plains (Allen, 1973; Harms et al., 1982)
Low-angle inclined stratified gravelly sandstone (facies GySix)	A few decimetres thick; a few metres wide; alternating layers (1–10 cm thick) of pebbly coarse-grained sandstone and medium- to fine-grained sandstone; each layer subparallel and low-angle inclined cross-stratified, showing a divergent fanning or offlapping pattern; strata generally conforming the lower topographic relief with tangentially or less commonly angularly downlap terminations; pebbles either flat-lying or imbricated; laterally juxtaposed with facies Glc or GySh units	Lateral or downstream accretion in bar fringes
Red–brown homogeneous or graded fine-grained deposit (facies Fh)	50 cm to more than 10 m thick; laterally continuous more than decametres; red to brown in colour; distribution-type graded with poorly sorted sandy siltstone bases and progressively well-sorted and weakly fissile siltstone tops; occasional oversized pebbles and cobbles; common calcareous nodules and vertical burrows; transitionally or abruptly overlying facies Gs or GZg units or stacked repeatedly by itself; occasionally including facies Gp units	Retarded suspension settling from weak floodflows (Turner, 1980; Jo, 2003)

Table 2
Characteristics and occurrence of architectural elements and facies associations

Architectural Element	Facies Association	Constituent Facies	Occurrence (Sections)	Along the eastern basin margin	Architecture and Stacking Pattern
Element I (alluvial fan)	FA IA (debris-flow-dominated fan)	Gt	B1–B5, G, H2	Along the eastern basin margin	Monotonous stacking of facies Gt units; discrete bodies along the eastern basin margin; partially radial dispersal pattern; preferential northeast to northwest-ward dipping. Progradational stacking of down-dip-thinning or -thickening bedset packages of facies GSs units; occasional foresets at down-dip margins.
Element II (ephemeral braided stream)	FA IB (sheetflood-dominated fan)	GSs, Glo	WG, I3		
	FA IIA (cut and fill)	Gtx, Glo	D, I1, I2, H1	Northwestern part of the basin	Sheet- or upward-widening-type geometry; sharp erosional base but diffuse gradational upper boundary; each body non-interconnected neither laterally nor vertically; encased within Element III deposits with interdigitating lateral margins; FA IIB dominant in the distal sections.
	FA IIB (low-relief bar)	Glc, GySh, GySix	SH, JH, HH		
Element III (channel-margin to floodplain)	FA IIIA (crevasse channel) FA IIIB (crevasse splay) FA IIIC (floodplain)	Glo, Glc, GySh, GySix Gs, GZg, Gp, Fh Fh, Gp	EG, I3–I5, H, JH, HH, Y, S3 EG, I3–I5, H, HH, Y, S1, S2, H1 SH, HH, I4, I5, Y, S1, S2	Western to central part of the basin; partly in the eastern basin margin	Finning-upward stacking of FA IIIA, FA IIIB and FA IIIC in ascending order; increasing proportions of FA IIIC in downstream direction accompanied with a decrease in frequency of FA IIIA and FA IIIB.

intercalations (Fig. 6). The conglomerate/sandstone couplets range in thickness from 20 to 50 cm and are generally laterally continuous for more than a few metres both in strike and dip sections (Fig. 6a, f). Each facies unit is mostly planar bedded, although the bases are very irregular with common downtruding clasts and local scoop-shaped scours (Fig. 6b, e, f). Some units are, however, partly cross stratified, forming either backset-stratified pockets (<28 cm thick and <3 m wide) (Fig. 6b, c) or stacked foreset-bedded complexes (each foreset <1 m high and total lateral extent >5 m) (Fig. 6d). Backsets involve a few reactivation surfaces and show an increase in dip angle (11 to 15°) and amplitude (18 to 28 cm) in updip direction, crossing the reactivation surfaces (Fig. 6b, c). Clasts are mostly of pebble to cobble grade with minor amounts of scattered boulders and are mostly angular to subangular. On the other hand, the lenticular conglomerates (facies Glo) usually occupy chute-like scour hollows of decimetres to metres wide and decimetres deep (Fig. 6b, c). It consists mainly of cobble-grade clasts with minor amounts of pebbles and occasional boulders that are tightly interlocked with open framework or with interstitial material of poorly sorted, fine- to coarse-grained sandstone. Occasionally, the hollow fills comprise crudely trough cross-stratified units conforming to the hollow geometry. The siltstone intercalations occur as erosional remnants of thin discontinuous wisps in the lower sections (Fig. 6b, c) but become thicker, laterally more persistent and more frequent toward the upper sections.

The conglomerate/sandstone couplets (facies GSs) consist of lower pebble-cobble conglomerate division and an upper division of pebbly, coarse-grained sandstone that are occasionally transitionally topped by laminated or unlaminated medium- to fine-grained sandstone (Fig. 6e, f). Each couplet generally forms a single sedimentation unit but in places, vertically superposed, two or more couplets constitute a single bed, revealing an overall fining- and thinning-upward trend (Fig. 6e, f). The lower conglomerate division is generally a-few-clast thick but the actual thickness is laterally variable due to local accumulations of coarsest clast fractions and lateral lensing. It is usually thickest (up to 20 cm) above scooped scours (Fig. 6b, e, f). It is either laterally persistent or discontinuous, comprising a few separate lenses that are generally more than 1 m wide and a few centimetres to decimetres apart (Fig. 6e, f). Sharp erosional bases are characteristic. Clasts are densely packed or clast supported with small amounts of matrix material that are almost identical in grain size and texture to those of the overlying sandstone division. Updip clast imbrication is common. The sharply overlying pebbly sandstone division is usually thicker than the conglomerate division unless truncated by the overlying bed. It consists of moderately sorted, granular sandstone and is either coarse-tail or distribution-type graded or ungraded (Fig. 6f). The associated pebble-size clasts are oriented either flow-parallel or flow-transverse and are commonly imbricated. They are either uniform, normally, or inverse-to-normally distributed. The occasional medium-grained sandstone top may comprise well-laminated, (sub-)parallel alternating layers of yellow to variegated medium sandstone and red-brown fine sandstone. Each bedset consisting of concordantly superposed beds of conglomerate/sandstone couplets commonly displays a fining- and thinning-upward trend (Fig. 6a, b).

Interpretation: The overall characteristics of the crudely stratified conglomerate/sandstone couplets (facies GSs) are very similar to those of the sheetflood deposits described by Blair (1987, 1999b, 2000), particularly in terms of the mode of stratification, clast size and packing, thickness and lateral extent of individual sedimentation units, development of erosional scours at the base, and the presence of scattered boulders. Blair (1999b, 2000) suggested that the planar couplets of pebble-cobble conglomerate and pebbly sandstone can be explained by successive bedload and suspension fallout deposition during the washout stage of sheetflood following

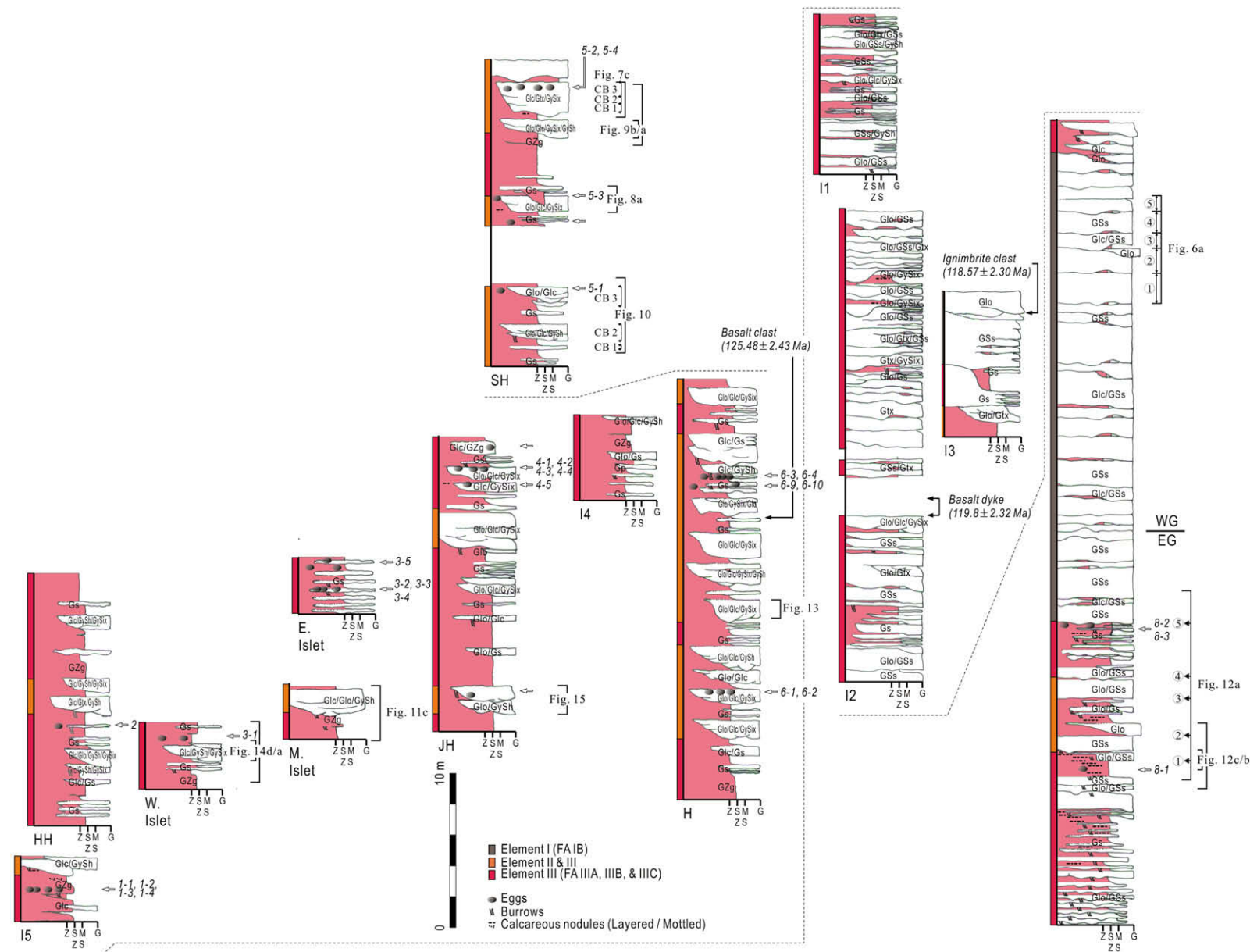


Fig. 4. Summary of columnar sections in the northern part of the Sihwa Basin. See Figs. 2 and 3 for the location of columnar sections. Stratigraphic correlation is based on both the bedding sequence and the location of dinosaur eggs (arrows with numbers). See Fig. 3b for the locality of egg occurrence. Facies codes are given. Columns are classified into three element groups, i.e., elements I, II and III, and III. See Tables 1 and 2 for details of sedimentary facies and elements. Z, SZ, M, S and C indicate siltstone, sandy siltstone, medium sandstone, and conglomerate, respectively. Note the gradual change of channel type in ascending order from the unconfined and flat-bottomed channels to the confined ones with V-shaped channel-walls as well as increase in both thickness of floodplain deposits and clast size in channel deposits. Dinosaur egg clutches generally occur in the uppermost part of the channel deposits or the overlying floodplain deposits, whereas solitary eggs occur on the bottom of channels. See Table 3 for detailed descriptions of egg occurrence.

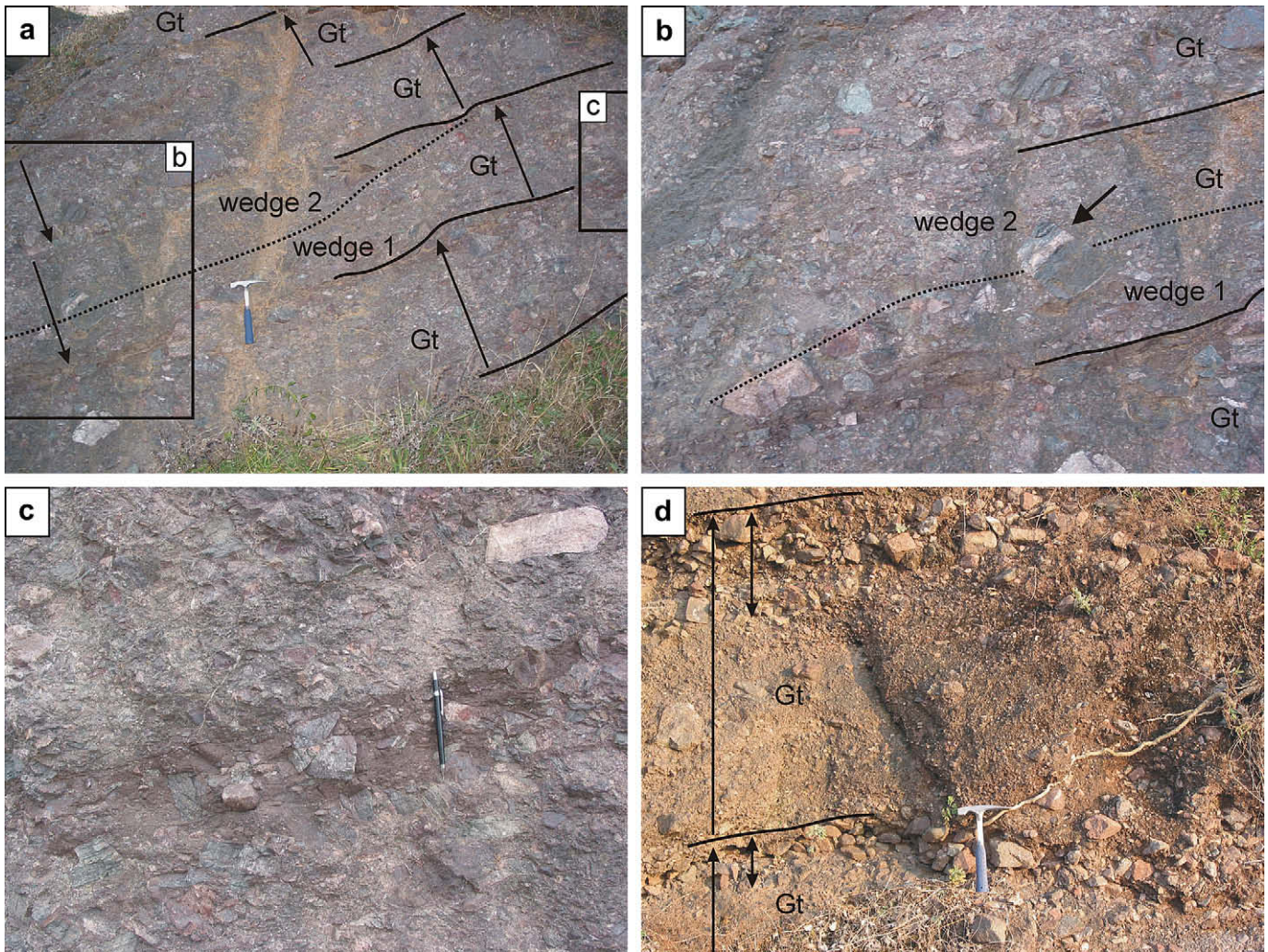


Fig. 5. Photographs of FA IA deposits of debris-flow-dominated fan. **(a)** FA IA consists of stacks of tabular conglomerates (facies Gt) with thin discontinuous red siltstone intercalations (from section B4). Note that a conglomerate bed consists of two overlapping wedges (see text for explanation). Upward arrows indicate inverse grading and downward arrows represent apparent but false normal grading. Hammer (30 cm long) for scale. **(b)** Enlarged photograph of part of (a), showing a superposition of the wedges. A large clast (arrowed) is not a floating clast in the middle part of the bed but a protruding clast above the lower wedge (wedge 1). **(c)** Enlarged photograph of part of (a), showing the intercalated siltstone lens. Note the irregular and diffuse lower boundary and the incorporation of pebbles. Pencil (14.5 cm long) for scale. **(d)** Inversely graded tabular conglomerates (facies Gt) with tightly interlocked clast-rich upper part (indicated by bidirectional arrows) (from section H2). Note that the interstices of clast-rich part remain void (openwork frame) or filled with finer-grained sediment, compared to matrix material of the other parts of the bed. Hammer for scale.

the breakage of supercritical standing waves. The clast-supported fabric, common clast imbrication and the thickening above scour surfaces of the conglomerate division confirm the bedload deposition and the common normal grading with no internal stratification in the sandstone division also corroborates the suspension deposition. However, intermittent bedload transport of gravel clasts is envisaged during the deposition of the sandstone division based on the fabrics of the associated pebble clasts. The occasionally laminated topmost part of the sandstone division suggests further bedload segregation during the late stage of suspension fallout. The occasional backset-stratified pockets indicate antidune deposition during the stage of standing wave development and/or subsequent wave propagation (Blair, 1999b, 2000). The updip increases in height and dip angle of backsets (Fig. 6b, c) suggest deposition by growing antidunes during an upslope propagation of standing waves with amplitude enlargement. The backset height of 18–28 cm may indicate flow depths of 27–56 cm, considering the flume observations of Simons and Richardson (1966) suggesting that water depth is 1.5–2 times the antidune height. The fining-upward bedsets of concordantly superimposed couplets may represent a successive cyclic deposition by repetitive formation and

breakage of standing waves and subsequent washout flows in a single-event sheetflooding (Blair, 1987). On the other hand, the scour-hollow-filling lenticular conglomerates (facies Glo) can be interpreted as gully-fill sediment formed during recessional flood or by secondary overland flows (Blair, 1999b, 2000).

It should be noted that the term “sheetflood” is used here for referring to a specific type of flood, i.e., unconfined and rapidly expanding, high-discharge, supercritical gravelly flood flow in which bedload and suspension sedimentation alternate. It was originally coined by geomorphologists to simply describe widespread floods that inundate almost all fan surfaces or tremendously large areas of floodplains, with little concerns on their hydraulics. Consequently, a wide range of flood processes have been included within this term (Hogg, 1982; Miall, 1985, 1996). Laterally extensive, centimetres to decimetres thick, ungraded or graded, laminated (partly rippled) or unlaminated, sand, sandy mud, or mud deposits (e.g., Mack and Rasmussen, 1984; Arguden and Rodolfo, 1986; Rhee and Chough, 1993a; Gómez-Villar and García-Ruiz, 2000) may represent an endmember-type sheetflood facies in the opposite end of the present deposit. These deposits can be viewed as formed by low-magnitude subcritical sheetfloods in which suspension

fallout sedimentation is prevalent with minor or no bedload traction. An intermediate-type deposit, e.g., massive to supercritically rippled (Boering and North, 1993a, b) or horizontal to low-angle cross-bedded (Tunbridge, 1981; Deluca and Eriksson, 1989; Marshall, 2000) sand sheets, may be formed by intermediate-magnitude, supercritical sandy sheetflood.

The overall predominance of gravelly sheetflood deposit (facies GSs) in FA IB suggests formation in a moderately sloping alluvial-fan environment (Blair and McPherson, 1994; Blair, 1999b, 2000). Based on the dominant depositional process, such a fan can be termed as “sheetflood-dominated fan”, differentiating from “debris-flow-dominated fan” of FA IA. The term “waterlaid fan” that is sometimes used for similar fan type (e.g., Blair, 1999b) seems inappropriate because it obscures the distinction from those fans largely constructed by braided streams (i.e., “streamflow-dominated fan”) (e.g., Harvey, 1984; Kochel, 1990; Ritter et al., 1993; Nemeč and Postma, 1993). In the present example, the fan succession is almost exclusively composed of facies GSs units with scarce backset-stratified deposits that have been commonly identified as an essential constituent of supercritical sheetflood deposits. This suggests that the FA IB deposit was most probably formed in the distal fan where intense washout flow erased almost all antidune remnants (e.g., Blair, 1999b, 2000). The relative thinness (< 2 m) of the composite bedset units also supports this inference. The foreset-bedded stacks (Fig. 6d) may indicate construction of micro-deltas, filling topographic lows at the fan margins by recessional floods or by overland flows during inter-flood stages.

3.2. Element II: ephemeral braided stream

Element II is characterized by multi-storey, sheet- or upward-widening-type, conglomeratic channel-fills whose maximum thickness exceeds 1.5 m (Figs. 7–10). It occurs mainly in the northwestern part of the Sihwa Basin (Sections D, I2, I3, H, SH, JH and HH), invariably encased within Element III deposits. Sheet-type channel fills are more common than the upward-widening types; the latter occur preferentially in the proximal sections (Sections D and SH). Each channel fill reaches up to a few metres in thickness and is laterally persistent over the entire outcrop (decimetres in lateral extent). The erosional base commonly involves numerous scours of more than 1 m wide and decimetres deep (Figs. 8 and 9). The upper boundary is generally transitional with an increase in thickness and frequency of the intercalated siltstone layers (Figs. 8, 9 and 10). Siltstone plugged scours are locally present along the upper boundary (Fig. 9). Lateral margins are rarely preserved in outcrops but interdigitating features with the encasing siltstones of Element III are observed at some places (Fig. 9). The channel bodies consist generally of singular or laterally and/or vertically superposed hollow fills (FA IIA) of openwork lenticular conglomerate (facies Glo) and trough cross-stratified conglomerate (facies Gtx) in the lower part and a composite deposit (FA IIB) of clast-supported lenticular conglomerate (facies Glc) and inclined or horizontally stratified gravelly sandstone (facies GySix and GySh) in the upper part (Figs. 8 and 9). Relative proportions of the former (FA IIA) to the latter (FA IIB) decrease downstream; the latter constitutes the whole channel body in the distal sections (Fig. 10). Gravel clasts are mostly pebble to cobble grade with minor amounts of boulders and are generally angular to subrounded.

3.2.1. FA IIA: cut and fill

Description: FA IIA is characterized by hollow-fill units with sharp erosional scoop-shaped bases. Each hollow is decimetres to metres wide (occasionally up to 3 m wide) and decimetres (up to 80 cm) deep. It forms a single isolated unit or more commonly

a laterally and/or vertically superposed composite unit. Solitary units display a narrow, scoop-shaped geometry with low width/height ratios in the range of 1–4 in strike sections. A unique outcrop section providing a horizontal view of the solitary hollow fill reveals the long and narrow chute-like 3D geometry with low-sinuosity planform. Hollow walls are mostly asymmetrical with the deepest axis near the steeper (up to 110°) flanks. Each unit is completely filled up by tightly interlocked, openwork lenticular conglomerate (facies Glo) or less commonly by low-angle trough cross-stratified gravelly sandstone or conglomerate (facies Gtx) above a basal veneer of one- to several-clast-thick facies Glo unit. Upward decrease in grain size is frequent in each case. Solitary hollow-fill units occur at the base and lateral margins of the channel body of Element II.

Composite units involving groups of superposed hollow fills are characterized by broader and shallower scour bases (width/height ratios of 4–10) than those of the solitary units. Symmetrical hollows are more common than asymmetrical ones; the latter are invariably laterally superposed at the steeper walls. The levels of deepest part of each hollow may ascend or descend in the next superposing one. Individual hollow fills are mostly composed of single sets of trough cross-stratified gravelly sandstones or conglomerates (facies Gtx) locally with minor amounts of openwork lenticular conglomerate (facies Glo) at the base. Cosets of facies Gtx with criss-crossing set boundaries are very scarce. Each hollow fill usually shows an upward-fining trend. The facies Gtx units consist generally of alternating layers of one- to several-clast-thick pebble-cobble conglomerate and (pebbly) coarse sandstone. Each layer is centimetres to 15 cm thick and inclined, conforming to the topography of a side of the basal scour surface with a maximum dip angle less than 15°. The conglomerate layer comprises tightly packed clasts with small amounts of interstitial material and frequently thickens toward the trough center or flanks. The sandstone layer involves moderately to well sorted, either massive or low-angle trough cross-stratified, granular coarse-grained sandstone. Laterally superposed composite hollow fills occur ubiquitous within the channel body of Element II, but concentrate in the lower part of the channel body, particularly at the deepest section. Such a complex of laterally and vertically superposed hollow fills is up to 2 m thick and is laterally persistent a few metres to decametres. Each hollow tends to become broader and shallower upward but the clast size is relatively constant.

Interpretation: The openwork lenticular conglomerate (facies Glo) is interpreted as channel-lag deposits (Nemeč and Postma, 1993), based on its occurrence above concave-up scour surface and the dense packing with scarce interstitial material. The trough cross-stratified conglomerate (facies Gtx) is, on the other hand, envisaged as resulting from successive pulses of bedload sheets (Whiting et al., 1988; Khadkikar, 1999). The low-angle (<15°) foreset dips and the scarcity of coset units negate deposition from three-dimensional (3D) dunes (Miall, 1977; Rust, 1978; Khadkikar, 1999). The alternate layering of conglomerate and sandstone can be explained by vertical accretion of longitudinally segregated bedload sheets, i.e., superposition of finer-grained tail over the arrested coarser-grained frontal part. The interstratification of the sandstone layer suggests development of low-amplitude bedforms after the removal (deposition) of coarse particles from the bedload. The general fining-upward trend in each trough set indicates a decrease in flow velocity at shallower topographic levels within a channel (Hubert and Forlenza, 1988) or waning floods (Stear, 1985).

Hollow fills of decimetres to metres scale have been interpreted as infills of minor channels or small scour pools (Miall, 1977; Rust, 1978; Jo and Chough, 2001). The common asymmetrical geometry of the solitary hollow fills with an oversteepened or overhanging wall is reminiscent of a cut-bank-like margin (Rhee et al., 1993),

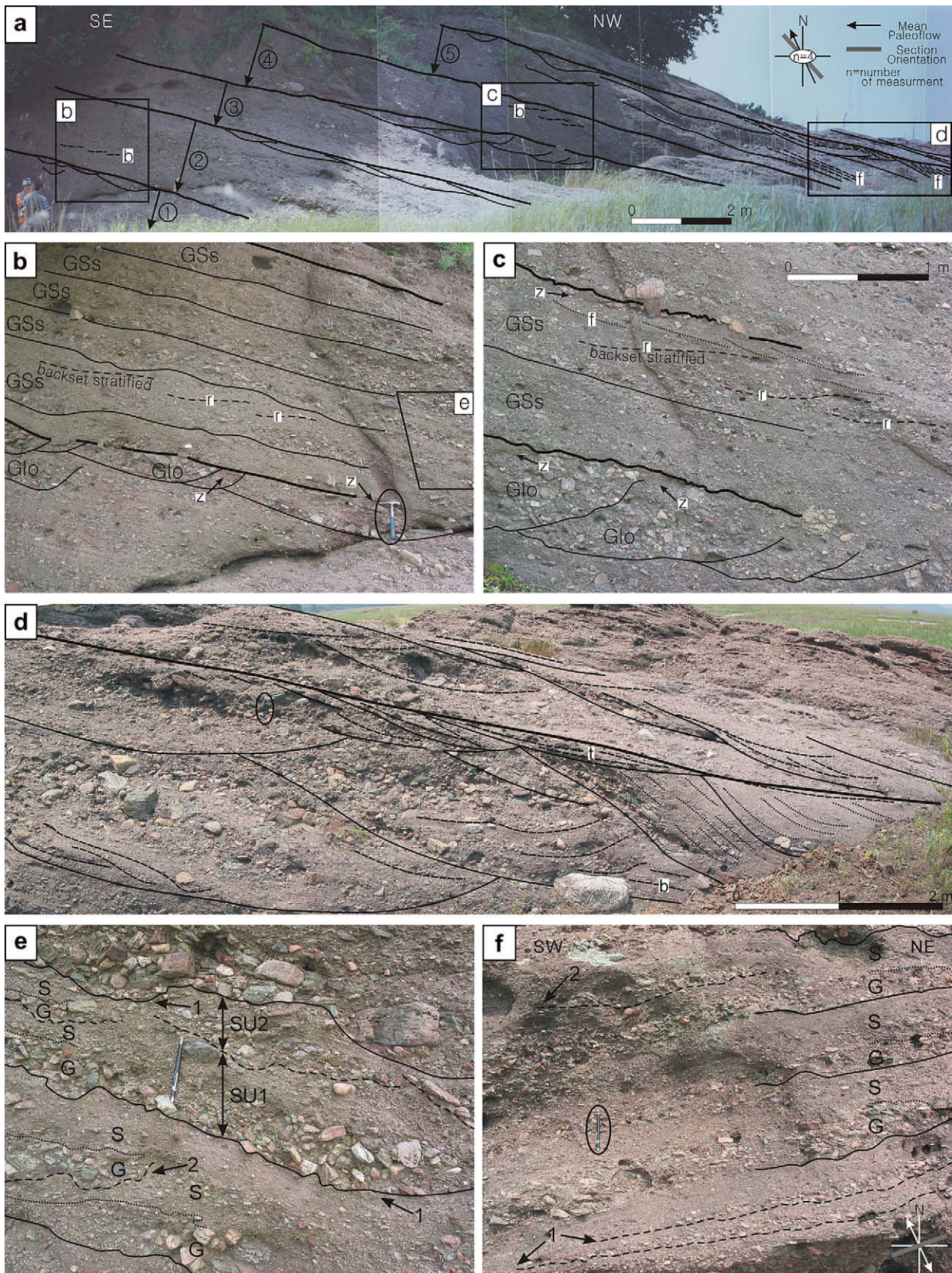


Fig. 6. Photographs of FA IB deposits of sheetflood-dominated fan at section WG (for location, see Fig. 3b). (a) A dip-section view. FA IB consists of progradational stacks of fining-upward bedsets of crudely stratified conglomerate/sandstone couplets (facies GSs) with minor amounts of hollow-fill units of openwork lenticular conglomerate (facies Glo), particularly along the tops of each bedset. Bedsets ①②③ & ⑤ thicken down-dip but bedset ④ thins down-dip. Note the foresets (f) at the down-dip margin of bedset ⑤ and the backset (b) stratifications in parts of bedsets ② & ④. Downward arrows indicate fining-upward trends. (b) Enlarged view of part of (a), showing the fining- and thinning-upward stacks of facies GSs units in bedset ② and the laterally superposed hollow fills of facies Glo along the top of bedset ①. Note the thin discontinuous erosional remnants of siltstone (z) at the bedset boundary. The backset-stratified unit involves a few reactivation (r) surfaces, marked by the change in mode of clast size and the dip angle. Hammer (circled) is 30 cm long.



Fig. 7. Photographs of large-scale channel-fill bodies (Element II) of braided streams. **(a)** Stacked channel-fill bodies intervened by crevasse splay and channel deposits (Element III) at Section D. Channel-fill bodies show either upward-widening (CB 1) or sheet-type (CB 2 and CB 3) geometry. **(b)** An upward-widening channel-fill body at Section SH reveals a dominance of cut-and-fill units (FA IIA) in the lower part and an abrupt transition into low-relief bar deposits (FA IIB) in the upper part. **(c)** Enlarged view of part of (b), showing the interdigitating feature in the right wing.

whose development necessitates channelized flows. The observed 3D appearance of a solitary hollow fill (Fig. 11f,g) clearly illustrates the elongated, chute-like geometry with a steep-sided wall along the outer curvature. The laterally superposed hollow fills are indicative of shifts in flow passages in discrete manner, which appeals to channel migration or switching. FA IIA is therefore interpreted as channel infills and their variations in dimension (width and depth) and stacking pattern most likely reflect the natural variability in the geometry and dynamics of channels, although the two-dimensional expression on outcrop surface is strongly dependent on the section orientation (i.e., depositional dip vs. strike faces). The solitary hollow fills may have resulted from instantaneous channel incision and subsequent rapid infilling, whereas the laterally and/or vertically stacked hollow fills would have formed by prolonged and multiple episodes of channel incisions with changing channel courses and gradual infilling through vertical and/or lateral accretions (e.g., Bridge, 1993; Leddy et al., 1993; Ashmore, 1993).

The complex units of FA IIA with vertically and laterally superposed hollow fills mimic cosets of trough cross-stratified deposits of 3D-dunes (Harms et al., 1982). Careful tracing of each erosional concave-up surface, however, indicates preferential lateral truncation rather than downcutting and the partial disconnection between hollow sets. These features deviate from typical configuration of set boundaries in 3D-dune deposits and can be

more satisfactorily explained by vertical stacking of laterally superposed channel fills. The upward transition into shallower and broader hollow sets also negates the 3D-dune origin because the height and width of dunes are genetically linked and show a strong co-variation (i.e., shallower the height, narrower the width). Khadkikar (1999) suggested empirical geometric criteria distinguishing troughs of channel and dune origin. The measured high width/height ratios (4–10) support the channel-fill origin, since dune troughs are characterized by lower ratios of 2–6 (Khadkikar, 1999). The vertical superposition of channel fills may reflect an aggradational river bed. In these respects, FA IIA is comparable to the “small-scale hollow fill” element of Jo and Chough (2001) and distinguished from their “trough cross-stratified set” element in case of the vertically and laterally superposed, complex hollow fills. Geometric configurations (width/height ratio and dip values) are suggested by Khadkikar (1999) and the descriptive details provided here may help this distinction.

3.2.2. FA IIB: low-relief bar

Description: FA IIB occurs in the upper part of the channel-fill bodies of Element II, sharply overlying the FA IIA deposits with planar erosional surface or occupies the entire channel-fill bodies in the distal sections. It comprises composite deposits of clast-supported lenticular conglomerate (facies Glc) and inclined or

(c) Enlarged view of part of (a). Note that the backsets increase in dip angle (11 to 15°) and amplitude (18 to 28 cm) in updip direction, and are draped by foreset (f) laminations. **(d)** Enlarged view of part of (a), showing a complex of foresets. Each foreset is based and truncated by concave-up surfaces, suggesting successive incisions and fillings of scour pools. Note the minor remnants of topsets (t) and bottomsets (b). **(e)** Enlarged view of part of (b), showing details of facies GSs units. Each facies unit is bounded by distinct erosional surfaces and consists of a lower conglomerate (G) division and an abruptly overlying upper division of pebbly sandstone (S). The conglomerate division is laterally variable in thickness, being thicker above scoop-shaped scours (arrow 1) and locally discontinuous (arrow 2). In some cases, a single bed comprises superposed subunits (SU1 and SU2) of facies GSs, showing an overall fining- and thinning-upward trend. Pencil (14.5 cm long) for scale. **(f)** A strike-section view. Planar configurations of each bed of facies GSs, likewise in dip-section view, suggest a tabular 3D geometry of individual depositional units. The tangential pinch-out (arrow 1) or lateral lensing (arrow 2) of stacked subunits in composite beds, however, indicate a genuine limit in lateral extensions during sedimentation.

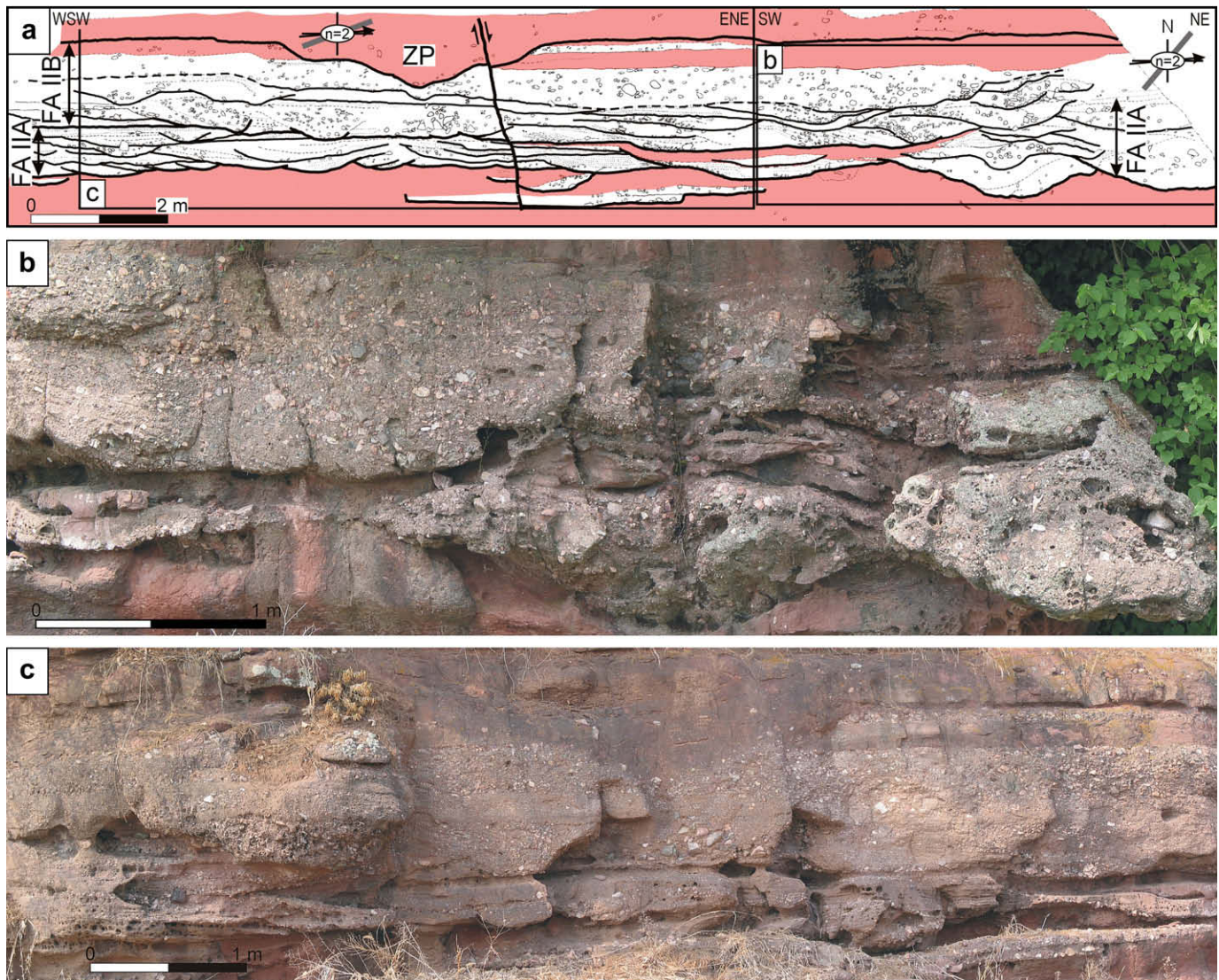


Fig. 8. (a) Line drawing of a sheet-type channel body (Element II) at the lowermost part of Section SH. The channel body consists of cut-and-fill units (FA IIA) in the lower part and low-relief bar deposits of FA IIB in the upper part. Note a siltstone-plugged (ZP) channel fill at the upper boundary. (b) (c) Photographs showing the parts of (a).

horizontally stratified gravelly sandstone (facies GySix and GySh) (Figs. 7–10). These units are either laterally or vertically stacked, showing complex arrangements and are locally bounded by sharp erosional surface with low-angle ($<10^\circ$) inclination and limited lateral extent of a few metres. Units of facies Glc and GySh are the most prevalent, whereas the units of facies GySix occur only in relative paucity.

The clast-supported lenticular conglomerate (facies Glc) is characterized by planar-convex, concave-planar or biconvex geometries and consists dominantly of pebble-size clasts with subordinate amounts of cobbles and boulders (Figs. 8–10). It ranges in thickness from 10 to 50 cm and is laterally continuous for a few metres, occasionally up to 20 m. In the lateral margins, beds are frequently transitional into inclined or horizontally stratified gravelly sandstones (facies GySix and GySh). Clasts are often concentrated in the thicker central part, forming a convex-up hummock in which clasts are disorganized and tightly interlocked. In relatively clast-deficient and finer-grained parts, pebbles are frequently imbricated and are locally normally graded or more commonly inversely graded. Matrix materials are composed generally of coarse-grained sandstone but in the central part, silty fine sandstone matrix is more prevalent.

The inclined stratified gravelly sandstone (facies GySix) is represented by a single set of low-angle cross-stratification in which each stratum generally conforms to the lower topographic relief (Figs. 9 and 10). Strata are subparallel and commonly show a divergent fanning or offlapping pattern in association with a downdip thickening of individual layers. Each layer angularly or tangentially downlaps onto the set boundary. The facies GySix unit occurs typically aside the clast-supported lenticular conglomerate (facies Glc), and is commonly laterally transitional into horizontally stratified gravelly sandstone (facies GySh). Accompanied with the facies transitions, a gradual decrease in clast size from the facies Glc through facies GySix to facies GySh units also frequently occurs. Each facies unit is a few decimetres thick (Figs. 9 and 10).

The facies GySh units are very similar in lithology to facies GySix in that both comprise alternating layers (ca. 1–10 cm thick) of pebbly coarse-grained sandstone and medium to fine sandstone. Each layer is (sub-)parallel, slightly undulatory or low-amplitude wavy and commonly diverges into separate layers. Lateral convergence into a single layer is also common. Low-angle ($<15^\circ$) internal scour surfaces are locally developed. Individual layers are either ungraded, normally graded or inversely graded and in places are interstratified. Pebbles are aligned parallel to the lamination and

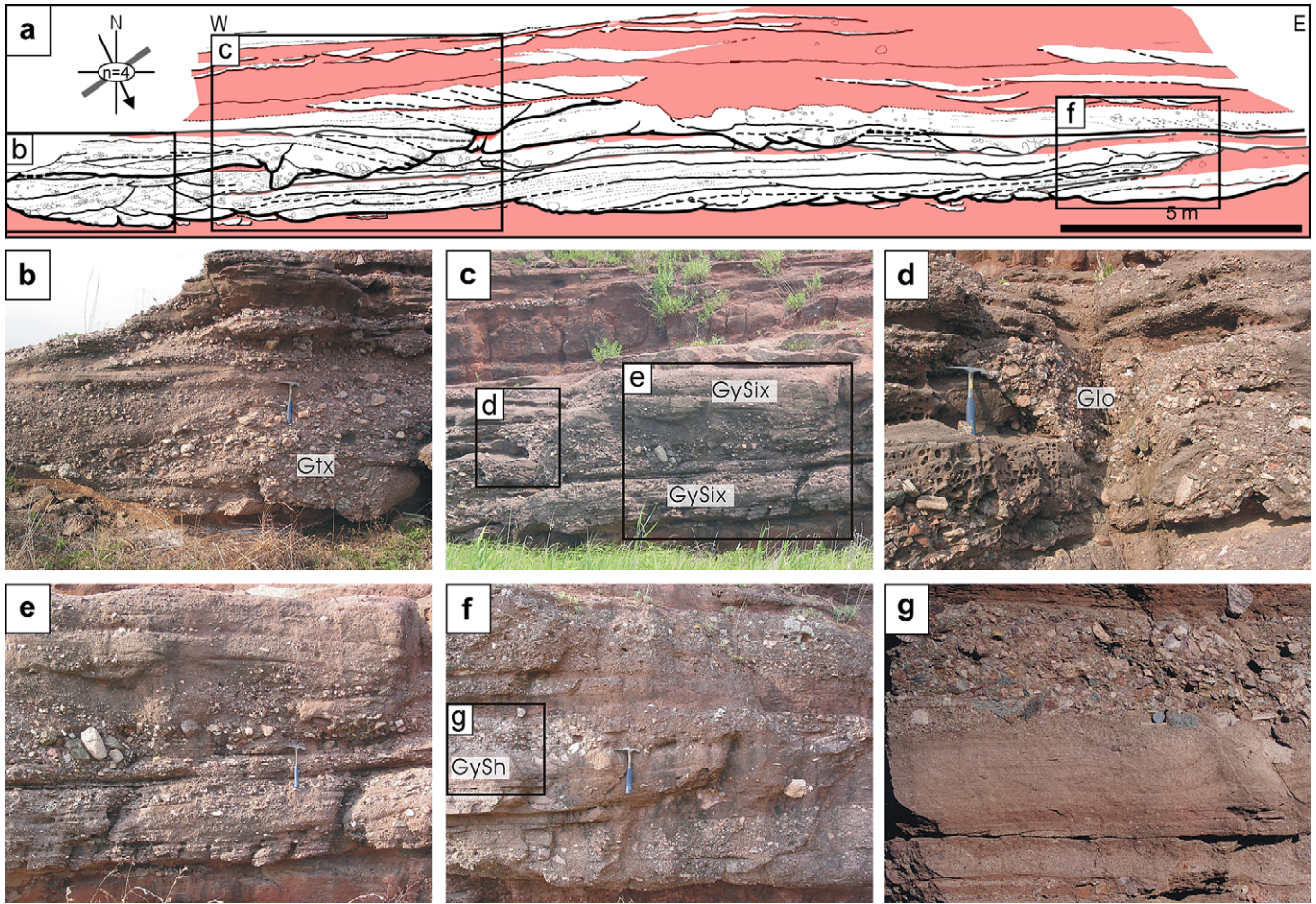


Fig. 9. (a) Line drawing of a sheet-type channel body (Element II) on the flow-transverse exposure at the upper part of Section SH. The channel body consists largely of cut-and-fill units (FA IIA) in the left part but low-angle inclined clinofolds or vertically stacked low-relief bar deposits of FA IIB in the right part. Note the interdigitating lateral margins (arrows). (b) (c) (d) (e) (f) Photographs showing detailed features of parts of (a).

are oriented either flow-parallel or flow-transverse, and commonly imbricated. Outsized cobbles and boulders are often associated. Each facies unit is a few decimetres thick (Figs. 9 and 10). Some units show an overall fining-upward trend.

Interpretation: The clast-supported lenticular conglomerate (facies Glc) is interpreted as low-relief longitudinal gravel-bar deposits (Boothroyd and Ashley, 1975; Miall, 1985; Karpeta, 1993; Jo et al.,

1997), on the basis of their common convex-up geometry, clast-supported fabric and generally disorganized nature. The lack of distinctive internal cross-stratification, the common up-flow clast imbrication and local inverse grading are representative of bedload transport by diffuse gravel sheets (Nemec and Postma, 1993). The laterally flanking, conforming strata of inclined cross-stratified gravelly sandstone (facies GySix) may indicate accretion in bar fringes. The horizontally

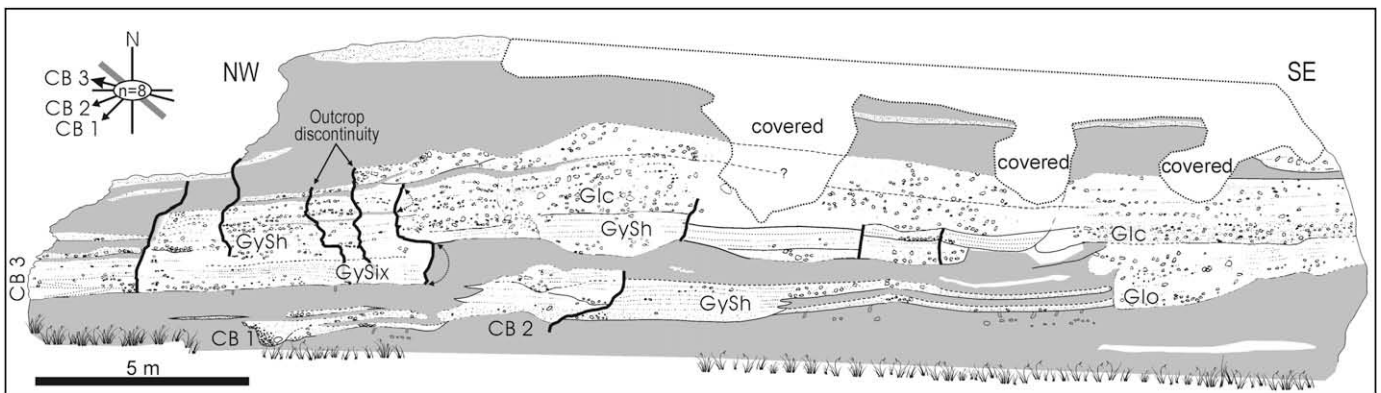


Fig. 10. Line drawing of a sheet-type channel body (Element II) on the flow-parallel exposure in the middle part of Section SH. The channel body (CB 3) consists mainly of vertical stacks of low-relief bar deposits of FA IIB with minor amounts of cut-and-fill units of FA IIA at the basal asymmetrical hollow in the right part. The bar deposit in the central part shows a downstream facies changes from unstratified conglomerate (facies Glc) to crudely stratified gravelly sandstone (facies GySh), while it displays a lateral lensing both in upstream and downstream direction. The underlying small-scale channel-fill units of FA IIIA (CB1 and CB2) indicates oblique to transverse palaeoflows, compared with that of the main channel body (CB 3).

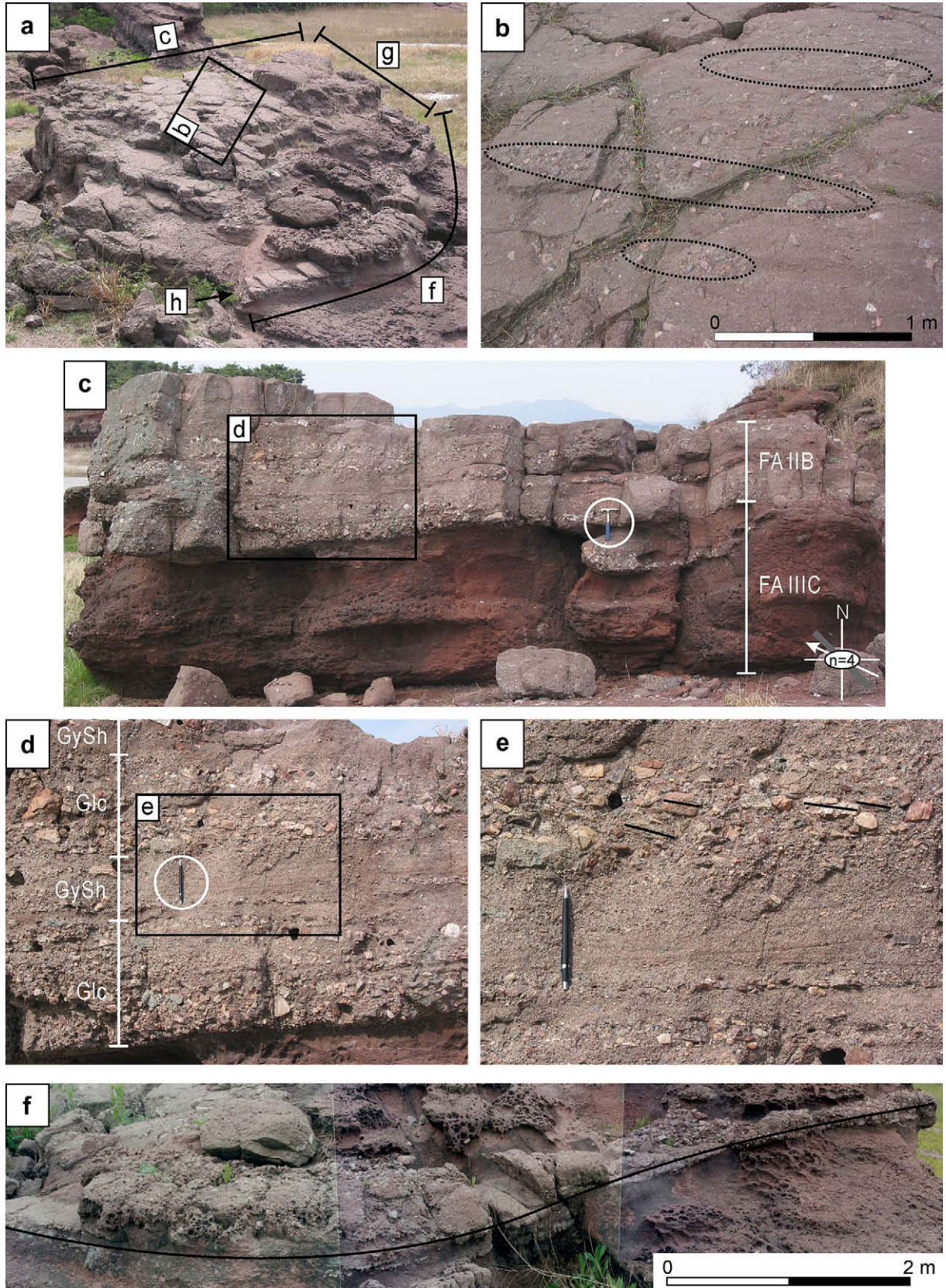


Fig. 11. Photographs of a 3D exposure of sheet-like channel body (FA IIB) with a narrow chute-fill (from an islet between Sections JH and HH). (a) Horizontal view, revealing juxtaposition of channel body and low-sinuosity chute-fill. (b) Enlarged view of part of (a), showing flow-parallel gravel clusters. (c) Vertical Section, showing the planar base of channel body above the floodplain fines. (d) Enlarged view of part of (c), showing dominance of clast-supported conglomerates (Facies G1c) and horizontally stratified gravelly sandstone (Facies GySh) in the channel body. (e) Note the clast imbrication indicating a westward flow direction. (f) Oblique view of chute fill. (g) Vertical section, showing the overlapping channel body above the chute-fill deposit. (h) Vertical section of the chute fill, showing the asymmetrical walls.

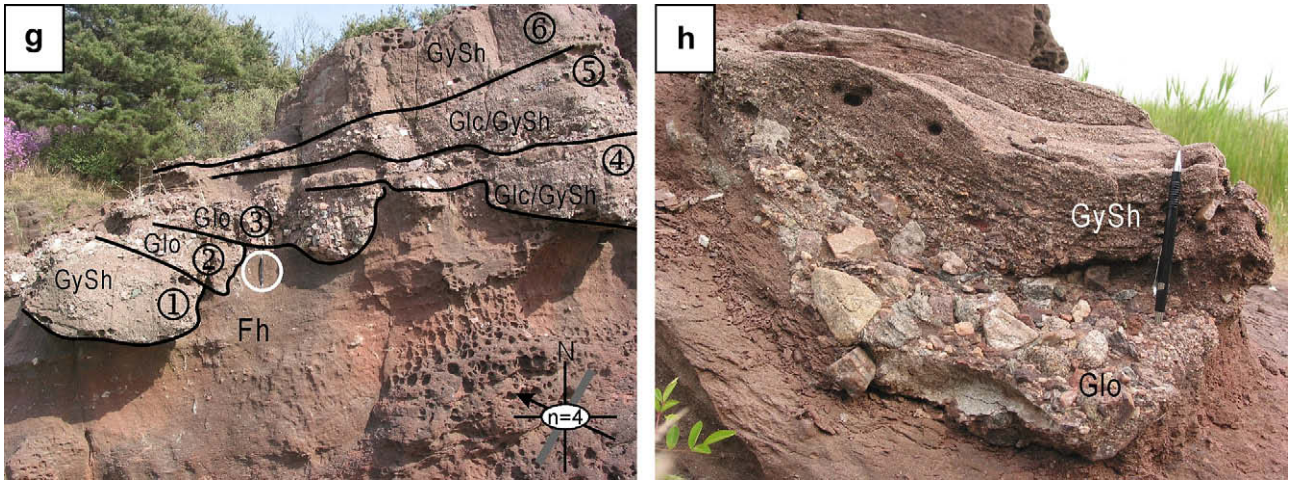


Fig. 11 (Continued).

stratified gravelly sandstone (facies GySh) suggests a broad, low-relief or plane-bedded bar (Allen, 1983), sand shoal or interbar plain. The (sub-)parallel to undulatory stratification with common layer convergence and divergence and local internal scour surfaces indicates development and migration of low-amplitude bedforms on the upper plane bed (Paola et al., 1989; Bennett and Bridge, 1995; Bridge and Best, 1997). Sedimentation of facies GySh units was probably coeval with the deposition of facies GySix units, given the common lateral juxtaposition of the two facies units. The overall characters of this facies association are very similar to those of the “stacked conglomerate and sandstone sheets” element of Jo and Chough (2001), except for the absence of trough cross-stratified sandstone.

The dominant vertical stacking of individual gravel-bar deposits with rare lateral superposition and scarce large-scale erosional truncations suggests an aggradational river bed with little changes in channel courses and consequently little bar migration. Each bar may have developed according to the cyclic impingement and dissipation of large-scale turbulence or surges of the flood flow. At the early stage of turbulence impingement and increasing shear velocity, all available clasts, regardless of their size, would have been actively entrained as bedload or bedload sheets (Whiting et al., 1988) by the flood flow. With the decrease in shear velocity due to the declining flow turbulence, bedload clasts begin to selectively deposit from the coarsest fraction that would form

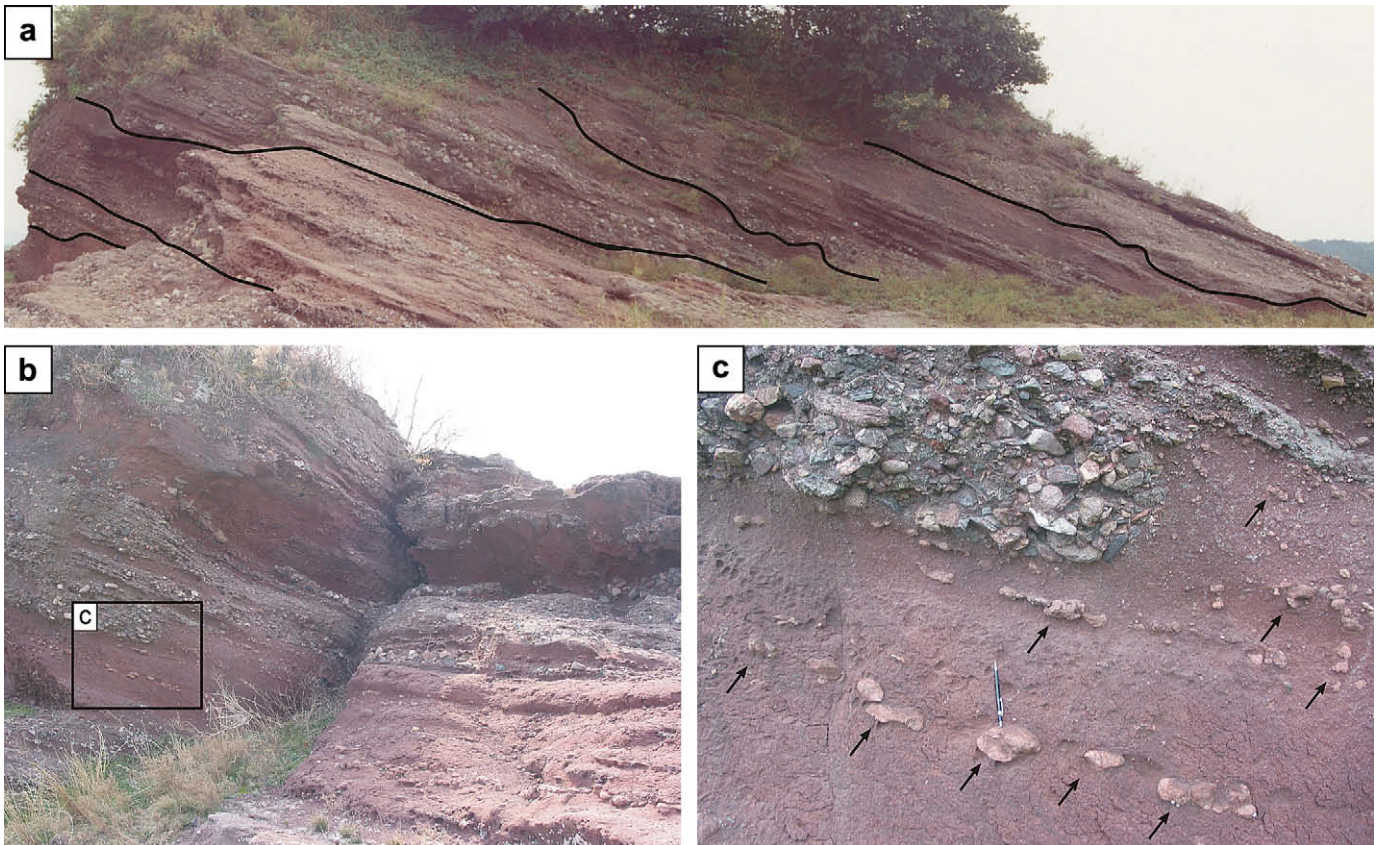


Fig. 12. (a) (b) (c) Photographs of a typical succession of Element III deposits, showing a fining-upward stacking of FA IIIA, FA IIIB and FA IIIC in ascending order (from Section EG). Arrows indicate concentrated horizons of calcareous nodules.

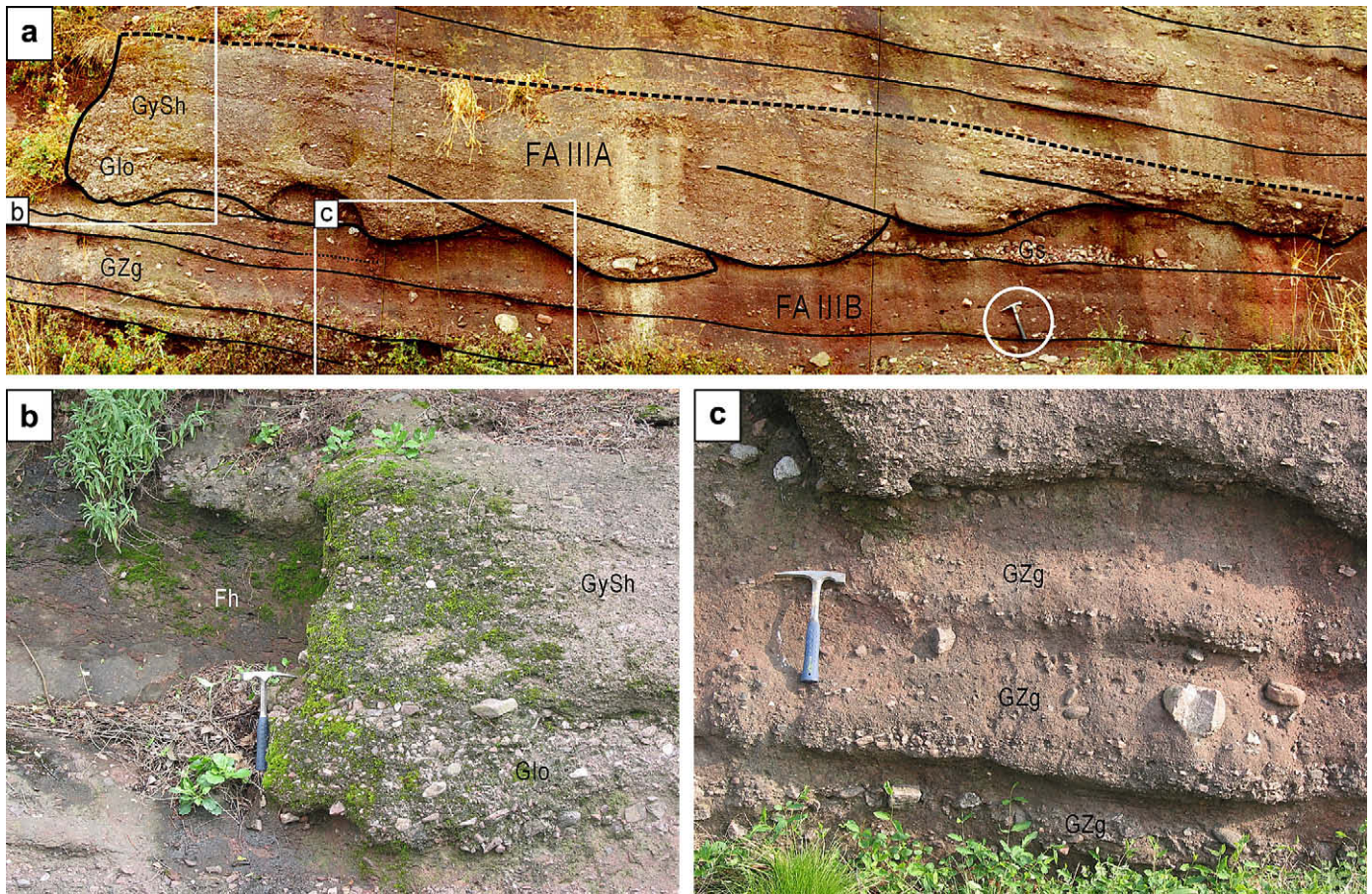


Fig. 13. (a) (b) (c) Photograph of a strongly asymmetrical, isolated, small-scale, single-storey channel-fill body of FA IIIA embedded in a FA IIIB succession comprising alternations of facies Gs and Fh units (from Section H). The corrugated features on the surface of fine-grained deposits can be ascribed to the differential weathering between silt and sand populations.

clusters and in turn grow as longitudinal bars by gathering finer clasts around them through blocking and attracting into the behind wake zone. The low relief of the bar deposit (facies Glc) can be explained by the delimited growth due to the subsequently lowering water level in the waning stage of the flood surges. The lateral sediment segregation from cobbly core to pebbly margins suggests selective entrainment of finer clasts into the renewed or continued, diffuse gravel sheets over the longitudinal bars. The laterally superposed inclined cross-stratified pebbly deposit (facies GySix) may represent reworked bedload deposition in the bar fringes at the lowering-water stage. The neighboring horizontally stratified sandstone (facies GySh) suggests coeval deposition of plane-bedded bars or shoals at the low-water stage. On the other hand, the cobbly hummocks in the central part of the bar deposit (facies Glc) are interpreted as the remnants of the initial bar cores, in which clasts are densely packed with a paucity of matrix material due to the selective deposition and continued stripping and condensing by the turbulent shears (Kim et al., 2003).

3.2.3. Discussion

The shallowness of each cut-and-fill unit, the absence of fining-upward lateral accretion packages and the development of multiple separate barforms in a flow-transverse section collectively indicate deposition in braided streams (Miall, 1977; Rust, 1978). The low-relief gravel and sand bars of FA IIB are products of peak flood flows with high water level, whereas the cut-and-fill conglomerates of FA IIA represent multiple erosion and filling processes in the channels between high-stage bars (FA IIB), probably after peak flood flows and during small discharge events. The

predominance of vertical stacking of low-relief bar deposits indicate repetitive deposition of the bars probably due to the cyclic fluctuations in flow velocity and water level in association with large-scale turbulence or surges in quasi-steady stage of flood. The gradual upward transition of Element II deposit into the Element III deposit with an increase in fine-grained intercalations indicates gradual abandonment of channels.

The downstream change of channel-fill geometry from upward-widening type to sheet type suggests that the distal part was less channelized, reminiscent of terminal fans (e.g., Sadler and Kelly, 1993). The simple organization of channel-fill architecture dominated with cut-and-fill and simple bar-resulting depositional packages as discerned in Element II deposit, together with the common fine-grained intercalations, is diagnostic of ephemeral braided streams formed by flash flows with high sediment discharge (Stear, 1983; Bromley, 1991; Jo, 2003). By contrast, perennial braided streams are generally characterized by complex channel-fill architecture consisting mainly of large-scale compound barforms with multiple accretion packages demarcated by erosional bounding surfaces, reflecting complicated history of intermittent growth, migration, superposition and coalescing of individual bars through multiple episodes of flood in a longer time span (Crowley, 1983; Luttrell, 1993; Jo, 2003).

3.3. Element III: channel margin to floodplain

This element is characterized by fining-upward stacks (up to 30 m thick) of (1) single- or multi-storey small-scale (<1.5 m thick) channel fills with limited lateral extent less than 15 m (FA IIIA,

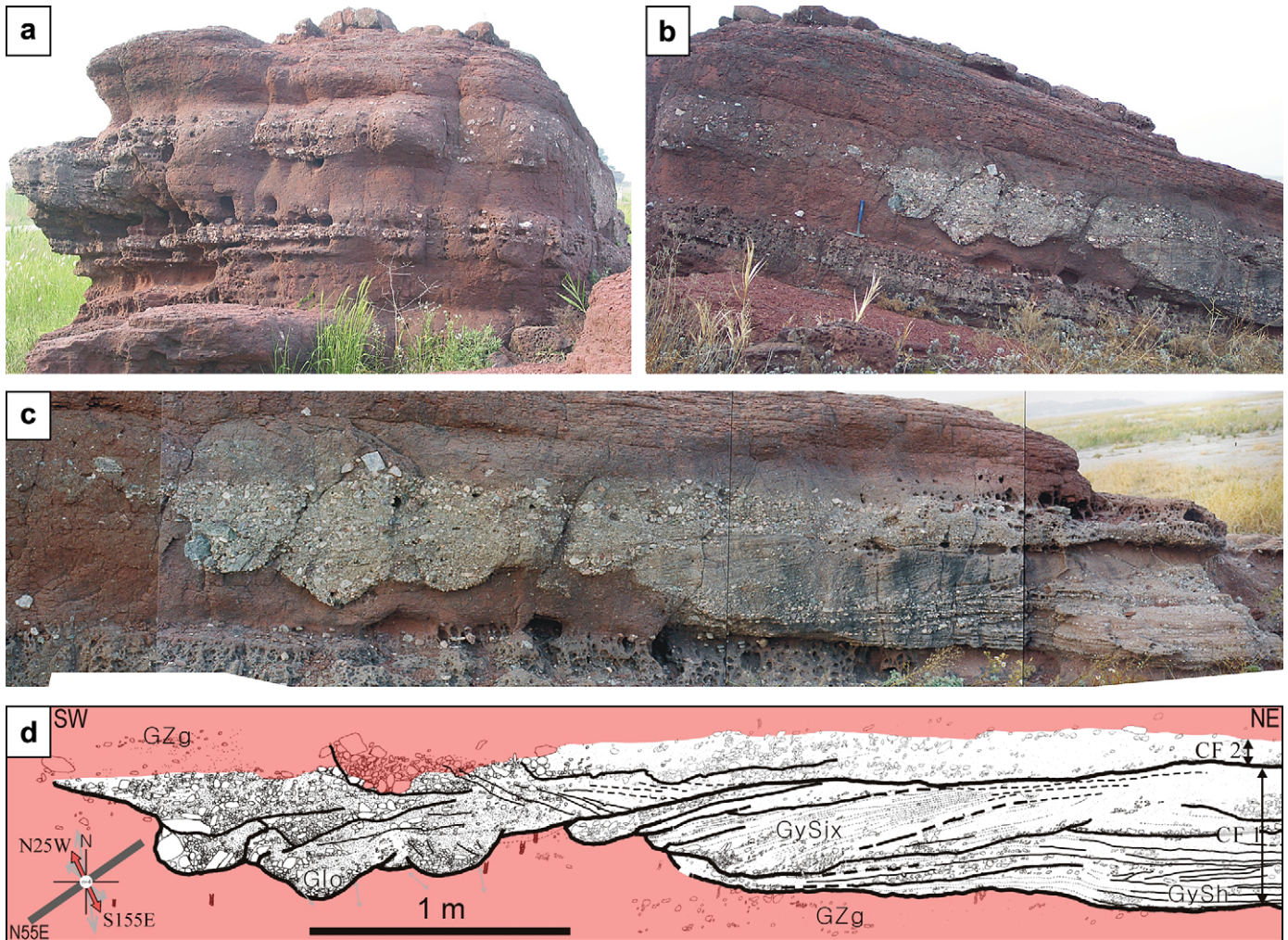


Fig. 14. Photograph (a) (b) (c) and detailed sketch (d) of a small-scale but multi-storey channel fill of FA IIIA embedded in FA IIIC deposits (from an islet between Sections JH and HH). CF: channel fill.

comprising facies Glc, Glo, GySi and GySh), (2) extremely poorly sorted, graded conglomerate/siltstone couplets (facies GZg) with diffuse gravel sheets or shallow hollow fills (facies Gs) (FA IIIB), and (3) poorly sorted, homogeneous or diffusely graded, red-brown fine-grained deposit (facies Fh) with gravel pockets or lenses (facies Gp) (FA IIIC) in ascending order. The deposits occur in most of western and central parts of the Sihwa Basin (Sections EG, H, SH, JH, HH, I4–I9, Y, S1 and S2), partly extending to the eastern margin (Section H2). In the northern basin, they are closely associated with Element II deposits in the transitional sectors between the FA IB deposits, whereas in the southern basin, they contact rather abruptly with the FA IA deposits, lacking intervening sections of Element II deposits. FA IIIA occurs dominantly in the northern transitional sectors (Sections EG, H, SH, JH, HH and I4–I9) but becomes absent toward the southern part (Sections G and S1–S3), where FA IIIB and FA IIIC are more prevalent. Thick-bedded units of FA IIIC develop in the central part of the basin (Sections Y, S1 and S2).

3.3.1. FA IIIA: crevasse channel

Description: FA IIIA is represented by single- or multi-storey small-scale channel fills that sharply scour the underlying fine-grained substrate (Figs. 12–14). The channel fills are generally more than 3 m wide with a thickness of less than 1.5 m, showing an overall bowl- or pan-shaped, symmetrical or asymmetrical geometry with smooth or slightly irregular bases and flat, rather distinct tops. In the proximal sections (Sections I1–I3, EG, and H),

each channel fill is single-storeyed with no internal bounding surfaces and shows a bowl-shaped geometry with a concave-up or broadly planar base and high-angle (60–90°) walls commonly with well-developed channel wings decimetres thick (Figs. 12 and 13). Its aspect ratio (width/depth) is between 2 and 4. These channel fills consist mainly of horizontally stratified gravelly sandstones (facies GySh) with minor amounts of openwork lenticular conglomerate (facies Glo).

In the distal sections (Sections H, I4, SH, JH, HH and I5), multi-storey channel fills (aspect ratio of 6–12) are more common with planar but locally scooped scour bases and steepened (30–60°), commonly stepped walls that are distinct in one side but diffuse on the other side (Figs. 13 and 14). Channel wings are absent. Internal bounding surfaces are prominent and preferentially inclined toward the distinctly bounded walls. Impingement of background fine-grained deposits along the internal bounding surfaces is common. Each channel fill is mostly isolated; in one place, vertically stacked channel fills show an upward decrease in dimension and grain size (Fig. 15). Internal channel-fill facies and architecture are very similar to those of the FA IIB deposit. That is, trough cross-stratified conglomerates (facies Gtx) commonly occupy the basal part and lenticular conglomerates (facies Glc and Glo) and stratified gravelly sandstones (facies GySh and GySix) occur above, showing a complex stratal arrangement. Individual channel-fills show, however, very different appearances; for example, one is dominated by units only of facies Gtx, whereas another consists merely

of units of facies Glo and GySix. The scarce internal chute-like scours and the common fining-upward internal grading distinguish themselves from those of FAIIB.

Interpretation: The close proximity of the channel-fill units of FA IIIA to the large-scale channel deposits of Element II and the characteristics of the constituent facies suggest rapid bedload deposition in channel margins or in the outlet of a channel branch. The distinct channel tops and the lack of vertically stacked internal units, however, preclude distally splitting distributary channels whose deposits are characteristically sheet-like with smooth, planar bases (Rhee and Chough, 1993a). The scour incisions of metre-scale depths with common overhanging and/or stepped walls preclude deposition by simple overflows and rather suggest crevasse channel incision (Rhee and Chough, 1993a; Rhee et al., 1993). FA IIIA is therefore interpreted as crevasse channels (Bridge, 1984; Rhee and Chough, 1993a; Rhee et al., 1993), whose dimension should be markedly smaller than the main trunk channels of Element II.

The single-storey units in the proximal sections with relatively low aspect ratio and the high-angle to overhanging channel wall indicate rapid channel filling by ephemeral flows during episodic events (Rhee et al., 1993). The predominance of horizontally stratified gravelly sandstones (facies GySh) indicates bedload deposition under upper flow regime. The well-developed channel wings further indicate an abrupt decrease in flow strength and thereby cessation of further channel incision and subsequent formation of overflows. On the other hand, the multi-storey units in the distal sections with relatively high aspect ratio and the preferentially inclined, shingled internal units suggest gradually migrating sinuous channels with cutbank-like margins at the distinctly bounded side (Rhee et al., 1993). The basal cut-and-fill units (facies Gtx) indicate initial channel incision and filling, whereas the overlying low-relief bar units (facies Glc and GySix) suggest sparse development of longitudinal bars during high discharge. The lack of channel wings suggests relatively well-confined channel flows with flow strengths enough to maintain continued channel incision.

The variation of overall geometry and architecture of individual crevasse channels can be accounted for by the proximity to the trunk channel; single-storey units in the proximal part to the main channel and multi-storey units in the relatively distal sectors. Crevasse channels are formed by bank failures along a trunk channel due to localized intense turbulent shear of flood flows. Outpouring, torrential flows would have undercut the substrate as deep as the level of the main channel and as wide as the breached gap in the bank. Subsequent channel filling was probably commenced with lag deposition and/or longitudinal gravel bars and then followed by sand deposition in the upper-plane-bed condition, as discerned from the vertical organization of constituent facies. In the proximal part with relatively high gradient, crevasse channels are quickly filled up and diverge in a discrete manner,

whereas in the distal part with lower gradient, channels are maintained for a longer period and gradually migrate with sustained channel flows (e.g., Rhee et al., 1993). The crevasse-channel origin is further supported by the palaeoflows measured from the channel walls that are nearly perpendicular to the palaeoflows estimated from the basal grooves, scour walls and the trough-cross stratification of the large-scale channel fills of Element II (discussed later).

3.3.2. FA IIIB: crevasse splay

Description: FA IIIB commonly occurs on top of the crevasse channel fills (FA IIIA) (Fig. 12). It consists of alternation of discontinuous gravel sheets (facies Gs) and fine-grained deposit (facies Fh) in the proximal part and stacked facies GZg units (coarse-tail graded conglomerate/sandstone/siltstone triplets and conglomerate/siltstone couplets) overlain by facies Fh unit in the distal part.

The gravel sheet (facies Gs) is characterized by densely packed, tabular or wedged gravel patch, a few clast to decimetres thick and laterally continuous in outcrop scale (>10 m in lateral extent) (Fig. 8b). Its lower boundary is relatively sharp and flat or concave-up in some places. The upper boundary is slightly convex upward or planar. Clasts range in size from pebble to cobble grade and are predominantly oriented parallel to bedding plane. Clast size frequently decreases toward the wedged margins. Beyond the wedged terminations, discontinuous pebble–cobble trains are commonly present. Matrix material is scarce in the central part and comprises moderately sorted, fine- to medium-grained sandstone. In the lateral margins, matrix proportions increase and become poorly sorted. Each gravel sheet commonly alternates with red–brown fine-grained deposit (facies Fh) decimetres thick, showing an overall thinning- and fining-upward trend. The composite units mimic the conglomerate/siltstone couplets of facies GZg but the densely packed, matrix-deficient fabric and the abrupt grain-size change to the overlying siltstone are distinctive.

Facies GZg units are diffusely or indistinctly bounded and are tabular bedded with a thickness of decimetres to more than 1 m (Fig. 13c). Each unit consists of lower pebble–cobble silty conglomerate division and an upper division of homogeneous or coarse-tail graded sandy siltstone, intervened by a middle division of silty sandstone. The conglomerate division is several clast thick, matrix- to clast-supported and partially stratified with local clast clusters. It is in places deformed and contorted in association with flame structures. Clasts are loosely packed and commonly imbricated. The matrix comprises sandy siltstone. The sandstone division is a few centimetres to more than 10 cm thick and consists of massive (ungraded and unstratified) or normally graded, moderately sorted, granular coarse-grained sandstone with matrix population of silt to fine-sand grade. The siltstone division is a few decimetres thick and comprises either coarse-tail or distribution-type normally graded, poorly sorted, non-fissile, red–brown sandy siltstone. Calcareous nodules or burrows are scarce. Individual beds

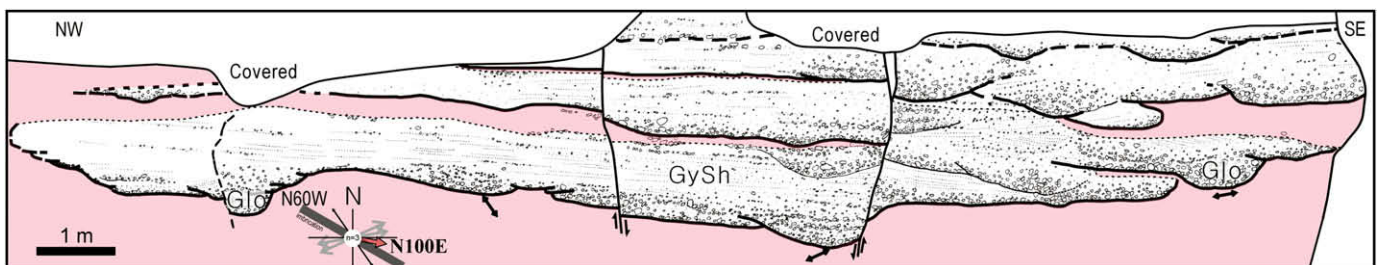


Fig. 15. Sketch of vertically stacked, small-scale, multi-storey channel bodies of FA IIIA (from Section JH). Each channel fill consists mainly of hollow fills of facies Glc and Glo in the lower part and transitionally overlying horizontal units of facies GySh. Bidirectional arrows indicate the axial directions of the scours at the channel base.

are usually stacked repeatedly, showing a fining- and thinning-upward trend. They are transitional upward into the succession of fine-grained deposit (facies Fh).

Interpretation: The close association of this facies association with the crevasse channel deposit of FA IIIA and the incorporation of large amounts of gravel clasts as coarse as those in the Element II deposits at numerous stratigraphic intervals suggest voluminous and repeated bedload supply from the main trunk channel. FA IIIB is therefore interpreted as crevasse splays (Stear, 1983; Mjøs et al., 1993; Rhee and Chough, 1993a; Bristow et al., 1999), which refer to a semi-conical deposit formed by outpouring floods through a crevasse in the breached levee or bank along the main trunk channel.

The facies Gs units formed by the pulsatory surges of the outpouring flood flows through the breached gap in the banks. The sharp erosional base indicates strong turbulence in the surge head. The dense packing, bedding-parallel clast orientation and the lateral continuation to discrete pebble–cobble trains indicate bedload deposition. The slightly convex-up upper boundary, common lateral pinching-out and the clast-size decrease toward the wedged margins suggest a low-relief splay-like form. This gravel facies unit is therefore analogous to the sand splays or sheets on the channel margins or floodplains (Mjøs et al., 1993; Rhee and Chough, 1993a; Jorgensen and Fielding, 1996; Bristow et al., 1999; Jo and Chough, 2001). The overlying fine-grained deposit (facies Fh) may have resulted from suspension sedimentation during the waning stage of each flood pulse. Absence of intervening deposits of intermediate-size sediment population can be accounted for by sharp sediment segregation within the flood flow due to strong fluid turbulence and bypassing toward the distal areas before flow collapses. Repeated alternation of facies Gs and Fh units showing a fining- and thinning-up trend suggests relatively frequent spillover probably due to the decrease in storage capacity of the main channel by aggradational filling and/or by repulsive flood surges with recurring intervals of flow waxing and waning.

The facies GZg units may have resulted from intermittent overflows or weakened flood flows in the distal areas because they are based with nonerosional surface and comprise relatively small amounts of gravel clasts. The relative paucity of gravel clasts, compared to gravel sheets (facies Gs) can be explained by the previous sedimentation in the proximal areas or by localized sediment supply from re-breached levees or river beds by episodic strong flood pulses after the original levee breaches were almost blocked. The basal conglomerate division with common imbricated clasts indicates bedload deposition, whereas the overlying normally graded sandy siltstone division represents subsequent suspension sedimentation. The fining- and thinning-up stacking pattern suggests a progressive decline in flow power in succeeding flood surges.

3.3.3. FA IIIC: floodplain fines

Description: FA IIIC is represented by red–brown fine-grained deposit (facies Fh), transitionally overlying the crevasse splay deposit of FA IIIB (Figs. 12–14). Each unit is commonly more than 50 cm thick and is laterally continuous over the entire outcrop (> decametres wide) with uniform thickness. It is commonly distribution-type graded with poorly sorted sandy siltstone in the lower part and the progressively well-sorted and weakly fissile siltstone in the upper part. Discontinuous granule–pebble lenses, trains or pockets (facies Gp) are common in the lower part and are either horizontal or slightly contorted and deformed. Some gravel pockets form tiny scour fills of decimetre-scale in width and depth. Outsized pebbles and cobbles are occasionally incorporated. Calcareous nodules or mottles are common in the upper part (Fig. 12c). Nodules are as large as 15 cm in diameter and in places concentrated in multiple horizons in a single bed. Vertical burrows (less than 5 cm in diameter and up to 20 cm long) are also common and

usually filled with sediment penetrated from the overlying bed. Each facies unit is usually stacked repeatedly, bounded by subtle scour surfaces that can only be discerned by sharp truncations of the tops of vertical burrows. This facies succession commonly shows an overall fining- and thinning-upward trend.

Interpretation: This facies association is interpreted as a flood-plain deposit, based on its occurrence on tops of and distal sections away from the crevasse splays of FA IIIB and the predominance of fine-grained deposits. Each unit of facies Fh was probably formed by the residual overflows of a single or several episodes of flood. The lower poorly sorted, sandy siltstone part indicates relatively rapid suspension sedimentation with minor tractive transport, whereas the upper part of more well sorted, fissile siltstone suggests retarded rate of suspension settling, probably from quasi-stagnant, slowly draining waters. The associated calcareous nodules and burrows indicate post-depositional modifications by pedogenic process and bioturbation, respectively. The red–brown colour reveals subaerial exposure and subsequent sediment reddening in an oxidizing condition (Friend, 1966; Turner, 1980; Retallack, 1997). Generally, red siltstone is formed in well-drained proximal floodplains, whereas gray siltstone is produced in the poorly drained, commonly waterlogged, distal floodplains (Jo, 2003).

3.3.4. Discussion

The spatial distribution and difference in structure and architectural arrangement of each component (FA IIIA, FA IIIB and FA IIIC) of Element III can be explained by the processes in the channel margins according to the difference in magnitude of ensuing flood pulse and/or the proximity to the main channel. In the proximal sections (Sections EG, I3 and H), low-aspect, single-storey crevasse channel-fills (FA IIIA) are overlain by or laterally juxtaposed with the crevasse-splay deposit (FA IIIB) dominated by interlayered gravel sheet (facies Gs) and thin fine-grained deposit (facies Fh) with rare poorly sorted gravelly siltstone deposits of facies GZg. The deeper channel incision, frequency of gravel sheets and the sharp segregation of grain size in splay deposits may indicate strong flood flows that were issued out of the main channel and thus were strongly turbulent enough to deeply scour and carry the bulk of sediment load far away, leaving only the coarsest bedload fractions. The interlayered fine-grained deposits indicate dumped suspended load during the waning stage of flood flows, before which intermediate-size sediment populations were already transported downflow. In the medial sections (Sections I4, SH, JH, HH and I5), high-aspect-ratio, multi-storey crevasse channel fills are common and associated with splay deposits dominated by poorly sorted, gravelly siltstones of facies GZg with less frequent and thinner gravel sheets (facies Gs) and thicker floodplain fine-grained deposit (facies Fh). The shallow and laterally migrating crevasse channels may have resulted from weakened flood flows in the distal areas from the main channel. These flood flows would have retained low erosional strength but continued longer period through multiple surges in the recessional stage of floods. Quick collapse of each surge as soon as it debouched and spread onto the floodplain resulted in poorly segregated splay deposits. Successive arriving of each surges would have partially reworked, deformed and buried the previous deposits, resulting in amalgamated units of facies GZg with sparse intercalations of diffuse and irregular gravel sheets, lenses and pockets (facies Gs and Gp). In the distal sections (Sections Y, H2 and S1–S3), metre-thick fine-grained deposits of facies Fh are dominant, occasionally associated with small-scale multi-storey channel fills (FA IIIA) and minor gravel sheets and pockets (facies Gs and Gp). The prevalence of relatively well-sorted fine-grained deposits indicates retarded suspension sedimentation in the floodplains during the slow draining of floodwaters. Occasional channel fills may suggest infrequent incision by extended crevasse channels or distributary channels. Associated gravel sheets or

pockets are probably analogous to those in crevasse-splay deposits in process. These coarse-grained deposits embedded in fine-grained floodplain deposits have been referred to as gravel (or sand) sheets or splays (Jorgensen and Fielding, 1996; Rhee and Chough, 1993a; Jo, 2003) with no critical evaluation on their difference in channel-margin crevasse splays.

4. Depositional environments and model

4.1. Palaeoflows and depositional environments

Fig. 16 summarizes the palaeoflow pattern and the distribution of each architectural element and the constituent facies associations in the Sihwa Basin. Alluvial-fan deposits (Element I) occur mainly along the eastern basin margin, forming three discrete sedimentary bodies. Debris-flow-dominated fans (FA IA) can be grouped into three distinct bodies: one is located at the southeastern basin margin (Sections B1–B5 and G) and the other two occur in the medial parts on the eastern margin (for example, Section H1). A partially radial palaeoflow pattern can be discerned from the former, based on the dip directions and clast orientation. One

sheetflood-dominated fan (FA IB) body is identified at the northern sector of the basin (Sections I2, WG and I3) and shows a north- to northwestward palaeoflow. These alluvial fans are regarded as basin marginal or basin transverse depositional systems issued from the eastern basin margin.

The braided-stream channel fills (Element II) occur in the northwestern part of the basin (Sections D, I1, H, SH and JH), showing interdigitating features with the enclosing gravelly siltstones of channel-margin and floodplain deposits (Element III). These channel fills display a southward palaeoflow and exhibit a downstream change in channel form from the upward-widening to sheet type, along with a decrease in relative proportions of the basal cut-and-fill deposit (FA IIA) to the overlying low-relief bar deposit (FA IIB). The associated channel-margin deposits also show a southward change in geometry of crevasse channel fills (FA IIIA) from a single-storey, bowl-shaped form with distinct wings to a multi-storey, asymmetrically shingled form with stepped margins. Scour axes of crevasse channels indicate a rather diverse palaeoflow, toward NW–SW or NE–SE direction, roughly perpendicular to those of the main channel deposits of Element II. The superposed splay deposit (FA IIIB) also shows a downstream

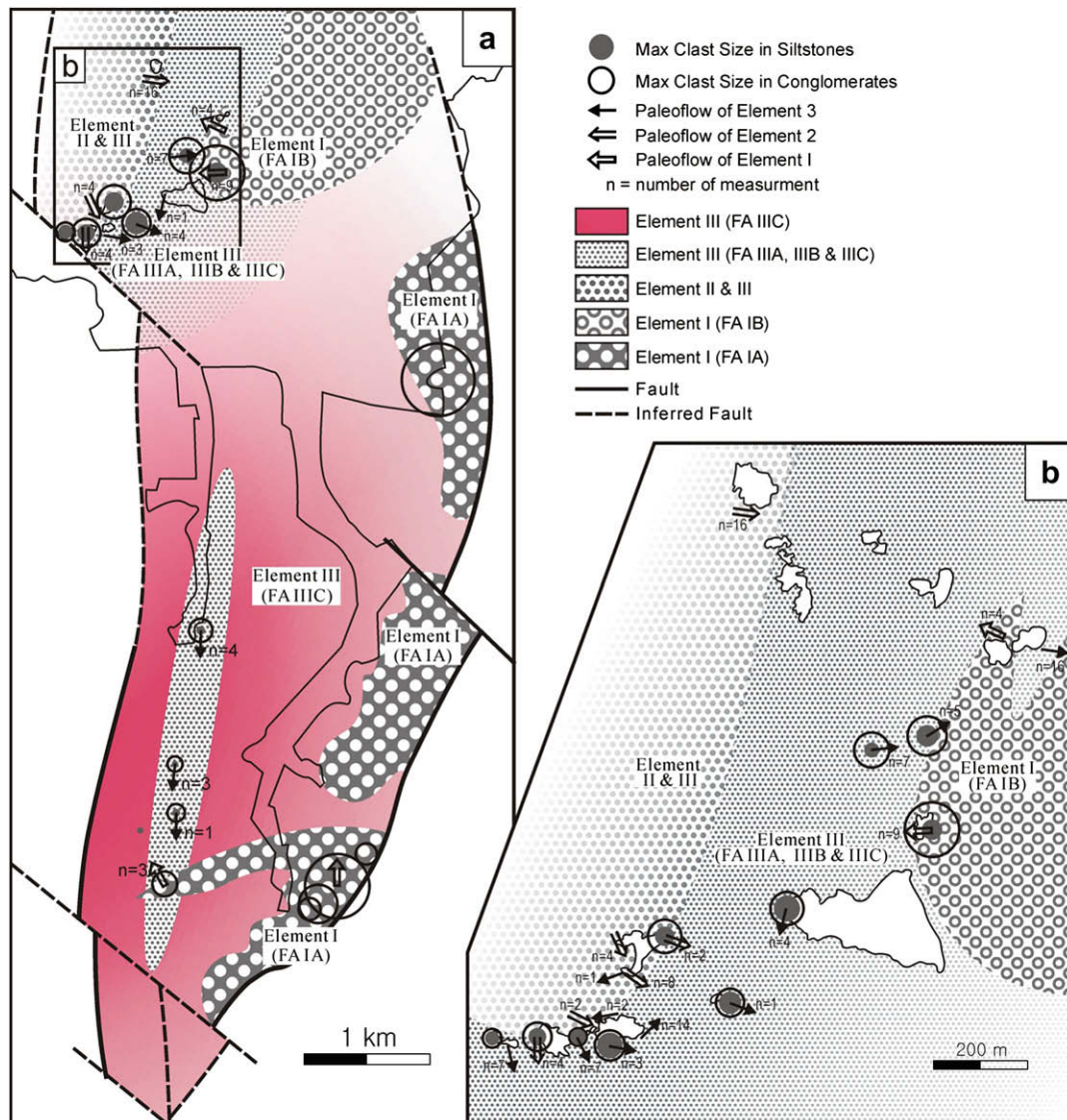


Fig. 16. Schematic map distribution of each element and facies association in the entire Sihwa Basin (a) and for the Hanyom area (b). Palaeoflows (measured from channel axis orientation and/or clast imbrications) and the maximum clast size (average of ten largest clasts) are also depicted by the arrows and the circles. Circle diameter is proportional to the clast size. Open circles represent the clast size in gravelly deposits, whereas the closed circles indicate the size of scattered clasts in silty deposits (facies GZg and Fh).

change in architecture, composed of alternation of gravel sheets (facies Gs) and fine-grained deposits (facies Fh) to stacks of poorly sorted, gravelly siltstones (facies GZg and Fh) with less common gravel sheets. Further downstream, floodplain fines (FA IIC) become overwhelming with sparse crevasse channel fills and gravel sheets in most of western and central parts of the basin (Sections I4, I5, HH, Y, and S1–S3) and partly in the eastern margin (Section H2). These downstream architectural variations indicate progressively less confined and diminishing braided streams with more common spillover but lesser crevasse incision in the distal part. The prevalence of red–brown floodplain fines in the basin center indicates a well-drained condition and poor development of lakes or pools. Such an indistinct termination of channel network is suggestive of a terminal-fan environment (e.g., [Sadler and Kelly, 1993](#); [Miall, 1996](#)). The southward facies transition from proximal braided stream gravels to distal floodplain fines with tied palaeoflow patterns and a decrease in clast size collectively suggest a basin-axial or basin longitudinal development of the terminal fan mainly along the western basin margin emanated from the northern end.

The juxtaposition of the basin-axial terminal-fan system with the basin-marginal alluvial fans is also corroborated by the distinct internal architectures and stacking patterns of the braided channel fills (Element II), which cannot be related to the braided-stream processes in the distal sectors of the alluvial fan. On alluvial-fan surface, braided channels form by lobe sedimentation and subsequent flow divergence at the termini of a trunk channel or chute beyond the intersection point between the channel floor and the fan surface ([Hooke, 1967](#); [Goedhart and Smith, 1998](#)). Lateral unconfinement and shallowness of flow is characteristic and thus the flow is invariably in the lower flow regime, resulting in preferential upstream and/or lateral accretion of lobes with no downstream avalanches and no channel-fill sedimentation ([Goedhart and Smith, 1998](#)). The resultant deposit is characterized by massive to crudely stratified, imbricated gravel sheets, representing annealed lobe remnants or composite braided bars ([Goedhart and Smith, 1998](#)). The common presence of cut-and-fill units (FA IIA), upper-flow-regime plane-bedded deposit (facies

GySh), and downstream accretionary bar fringes (facies GySix) in Element II therefore disprove an alluvial-fan setting. The low flow depth/grain size ratio and the absence of gravel bedforms with avalanche faces are indicative of less or unconfined, shallow flows but do not necessarily indicate a steep-gradient environment (e.g., [Heinz and Aigner, 2003](#)).

4.2. Depositional model

The sedimentary fill of the Sihwa Basin can be divided into two depositional successions: the lower terminal-fan succession distributed widely in the western and central parts of the basin and the sharply overlying alluvial-fan succession forming discrete bodies along the eastern margin. [Fig. 17](#) depicts a two-stage evolution of the Sihwa Basin. The terminal-fan succession is characterized by an aggradational stacking pattern, i.e., each channel fill of the proximal braided stream is vertically superposed, not being interconnected but demarcated by the intervening channel-marginal to floodplain fine-grained deposits. The basin-marginal alluvial-fan successions are characterized by a progradational stacking pattern preferentially in a northward direction despite the partially radial dispersal pattern. The overall basin-fill architecture and the variations in stacking pattern of each succession can be understood in terms of the interplay of basin subsidence (tectonics) and sediment supply (e.g., [Leeder, 1995](#)).

The aggradational stacking pattern of the lower terminal-fan succession suggests relatively rapid subsidence of the basin floor at a rate exceeding or balanced with sediment supply rate in the early stage of basin formation. The southward dispersal pattern and the basin-wide distribution of fine-grained deposits suggest an abundant sediment supply from the drainage basin with large catchment areas and high-order drainage networks beyond the northern basin end. Generally, a basin-axial system is fed by the largest drainage basin among others and thus forms a widest depositional unit ([Gawthorpe and Colella, 1990](#)). In contrast, the progradational stacking pattern of the upper alluvial-fan succession indicates retarded rate of basin subsidence below the sediment supply rate in

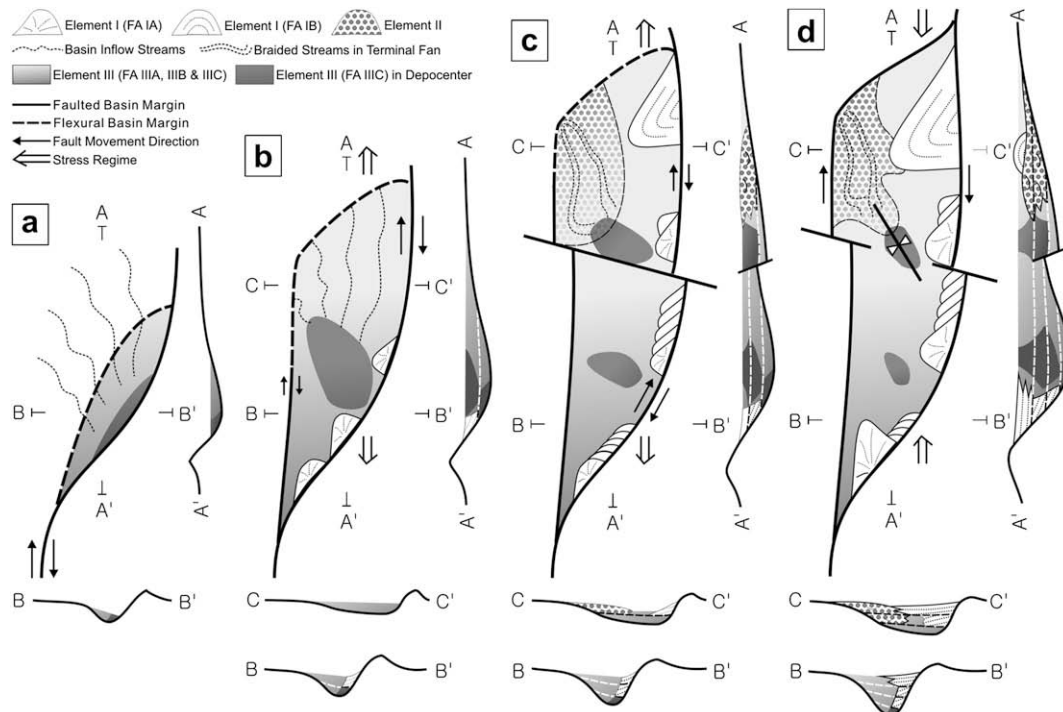


Fig. 17. Reconstructed evolution model of the Sihwa Basin.

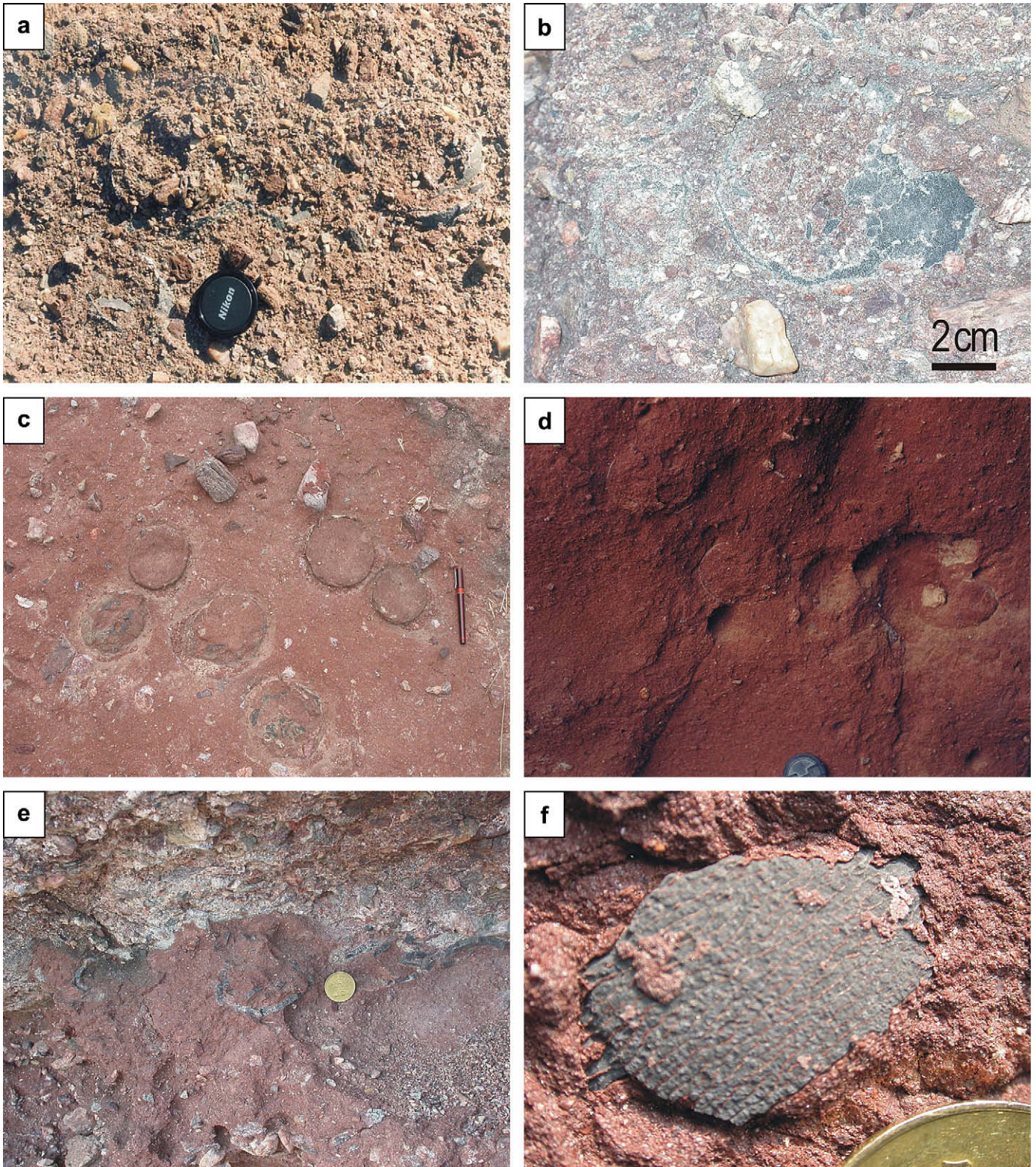


Fig. 18. Intact oval-shaped dinosaur eggs filled with substrates, which occur mainly together up to several units in the same horizon and repeatedly in different stratigraphic horizons. Lens cap (5.5 cm in diameter) for scale. **(a)** Topless eggs in trough cross-stratified conglomerate at Sanghanyom. **(b)** Topless eggs in tabular conglomerates at Sanghanyom. **(c)** Concentrated dinosaur eggs in gravelly siltstone at Joonghanyom. Pen (13 cm in length) for scale. **(d)** Dinosaur eggs in slightly gravelly siltstone at is Lens cap (5.5 cm in diameter) for scale. **(e)** Type 2 dinosaur eggs in gravelly siltstone at Gaemisum. Coin (2.3 cm in diameter) for scale. **(f)** Enlarged view of the shell surface of Type 2 eggs. Coin (2.3 cm in diameter) for scale. For locations, see Fig. 3.

the late stage of basin evolution. Reduced accommodation space is prerequisite for activation of marginal fans and permits their areal expansion (progradation) (Gawthorpe and Colella, 1990). Discrete form of each alluvial fan suggests separate drainage basins of small

size along the eastern basin margin. On the other hand, the overall asymmetrical cross-basin distribution of depositional systems with gravelly alluvial fans in the eastern basin margin and a floodplain in the western margin reflects a half-graben structure of the basin

with steep-gradient fault-bounded eastern margin (footwall block) and gently sloped flexural western margin (hangingwall block) (e.g., Crowell, 1975; Gloppen and Steel, 1981; Leeder, 1988; Gawthorpe and Colella, 1990).

The changes in rate of basin subsidence in a transtensional basin are ascribed to the temporal variations in relative magnitude between strike- and dip-slip rates on the basin-bounding faults (Schubert, 1980; Frostick and Reid, 1990). Accordingly, it is conceived that dip-slip motion of the eastern basin-bounding fault had a high rate in the early stage of development of the Sihwa Basin but decreased and was surpassed by the lateral slips in the late stage. The early-stage basin-axial deposition of a terminal fan system cannot however be directly linked to the fault movement in the eastern basin margin. It may need to presume an activation of transfer faults along the northern basin end at the tectonic peaks of the eastern boarder fault, considering the common linkage of the development of basin-axial system with transfer fault movement in transtensional basins (e.g., Crowell, 1975; Steel and Gloppen, 1980; Gawthorpe and Colella, 1990; van der Straaten, 1990). The late-stage basin-marginal deposition of alluvial fans was probably affected by the sinistral movement on the eastern strike-slip fault, given the preferential northward stacking pattern of the alluvial-fan deposits, since basin-marginal alluvial-fan bodies are skewed in the direction opposite to that of the basin-floor displacement (e.g., Crowell, 1975, 1982; Steel and Gloppen, 1980; Nilsen and McLaughlin, 1985; Steel, 1988).

4.3. Palaeoclimate

The predominance of ephemeral braided streams along with the red-brown floodplain deposits with common calcareous nodules in the Sihwa Basin indicates an arid to semi-arid palaeoclimate. This climatic condition is favorable for the development of ephemeral braided streams because the seasonally concentrated precipitations, poor vegetation, and ample production of coarse-grained colluviums during the dry seasons are all beneficial for triggering high-discharge flashy flows (Stear, 1983; Bromley, 1991). Broad and shallow channel incision and subsequent rapid channel filling are characteristic of ephemeral braided streams. The lack of perennial discharge is indicated by scarcity of modified features along the tops of the preserved simple bars and the absence of large-scale compound barforms (Crowley, 1983; Luttrell, 1993; Jo, 2003). The development of calcareous nodules on the floodplain deposits also suggests an arid to semi-arid palaeoclimate, since its formation requires prolonged excessive evaporation (Steel, 1974; Retallack, 1997). A warm and arid to semi-arid climate in the Korean peninsula during the Cretaceous has been widely recognized by the occurrence of distinctive palynological assemblage (Choi, 1985), pedogenic characteristics (Paik and Chun, 1993; Paik and Lee, 1998; Paik and Kim, 2003), terminal-fan facies assemblages (Rhee and Chough, 1993b) and the distinctive sedimentary deposits, such as radial calcite oolite embedded in lacustrine stromatolite (Woo et al., 1991) and inorganic hydrogenous lacustrine chert (Chough et al., 1996).

5. Dinosaur eggs and nests

Based on detailed taxonomic studies on dinosaur eggs in the Sihwa Formation, the eggs are classified into two types (Lee et al., 2000). Type 1 eggs (black in colour) are characterized by large size (11–15 cm in longest diameter) and a thin shell (0.85–1.23 mm), whereas type 2 eggs (dark gray to black) are of small size (9.5–10.3 cm in longest diameter) and a thick shell (3.4–5.0 mm). Both types are characterized by spherical to subspherical shape, absence of surface protuberance or ornaments and an abundance of open pore canals (ca. 50% of the surface area), i.e., dinosauroid-

spherulitic type (Hirsch, 1994), characteristic of herbivorous dinosaurs. The pore canal structure and inner shell surface texture, however, show different characters. Type 1 eggs are characterized by depressed circular openings (0.34–0.45 mm in diameter) in the outer surface and interconnected beneath, forming labyrinth-type network with no linear columns in vertical section. The inner shell surface is smooth and unpatterned. Type 2 eggs comprise longitudinal, wavy, and commonly bifurcating furrows or striations (sub-millimetre wide and av. 0.8 mm apart) on the outer surface and show wedge-shaped, outward fanning and bifurcating columnar canals with faint growth lines in vertical section. On the inner surface, polygonal or circular mammilla blocks are developed, compartmented by surrounding canal openings.

The Type 1 eggs belong to the filispherulitic morphotype and can be referred to Faveoolithidae (Zhao and Ding, 1976), whereas the type 2 eggs represent a dendrospherulitic morphotype and the Dendroolithidae (Zhao and Li, 1988). The former is further assigned, based on the primitive, irregular patterns of pore canals, as *Youngoolithus xianguanensis* (Zhao, 1979), which implies deposition during the Early Cretaceous (Lee et al., 2000). Eggs of Faveoolithidae have been identified as those of sauropods (Zhao and Ding, 1976). The common multicanalliculate pore system of both type eggs suggests that the eggs were laid and buried under moisture soils or ground (Lee et al., 2000). However, most eggs are regarded as unhatched due to the absence of respiration craters on the inner surface (Lee et al., 2000).

More than 140 dinosaur eggs, either isolated or clustered, have been identified from several stratigraphical horizons (Figs. 4 and 18; Table 3). They mainly occur in the cut-and-fill conglomerates (facies Gtx) of the main channel (FA IIA) or crevasse channel (FA IIIA), and gravely siltstones (facies GZg) of the crevasse splay (FA IIIB) deposits. The eggs commonly form concentrated horizons of 2–6 eggs in vertical section and are locally arranged in a circular pattern (ca. 50–60 cm in diameter) in plan view, which strongly appeals to intact preserved clutches (Lee et al., 2000). These are indicative of the dinosaur nesting habits in floodplains and abandoned channels (e.g., Erben et al., 1979; Iatzoura et al., 1991; Cousin et al., 1994). The eggs are, however, completely stuffed with the substrate of gravels and silt, either breached or holed, although the original oval shape is retained, suggesting that the egg-bearing deposits formed mainly during flood events.

Sauropod nesting habitats are recognized by laying eggs in a pit and burying egg with sediment or vegetation (Sanz et al., 1995). Moisture is required for multicanalliculate type eggs in generally semi-arid to arid climatic conditions. Preferential nesting habitat should be located to the near-channel or abandoned channel areas. The occurrence of stuffed substrates in within-channel deposits suggests that sauropods chose channel floor in the distal alluvial fan as nesting habitats during dry season. The abundant yield of eggs, more than 10 eggs in a single depositional unit, is suggestive of a dense dinosaur population. These horizons reflect site fidelity as a nesting habitat of near-channel or abandoned channel areas.

6. Conclusions

The Sihwa Formation (Cretaceous, mid-west Korea) consists of ca. 3-km-thick non-marine succession that can be classified into three architectural elements, representing distinct depositional environment: (1) alluvial fan (debris-flow-dominated or sheet-flood-dominated fan), (2) ephemeral braided stream and (3) channel margin to floodplain. Four depositional systems are identified from the distribution of the architectural elements: two debris-flow-dominated alluvial fans in the southeastern basin margin, one sheetflood-dominated fan in the northeastern margin and one terminal fan in the northwestern margin. The latter comprises ephemeral braided streams in the proximal part and distributary

Table 3
Occurrence of dinosaur egg fossils in the Sihwa Formation

Location	Nest Size (cm ²)	Egg type (diameter, cm)	Number of eggs	Characteristics of occurrence
1-1 I5	273	1 (12)	9	Distributed linearly in a distance of 30 to 70 cm apart in reddish sandy siltstone layer. Top part of every egg is open and shell fragments accumulated at the bottom. One egg shell is filled with sandy silt and gravels at the top and sandy silt in the rest.
-2	77	1 (11)	3	Distributed in a linear fashion, 20 to 30 cm apart
-3	-	1 (10)	1	Occurs with a lot of shell fragments
-4	25	1 (10, 13.5)	2	Aggregated with a lot of shell fragments
2 HH	-	1 (8)	1	In reddish sandy siltstone with shell fragments
3-1 Islets between	15	1 (15 × 2.3)	3	Egg shells are flattened, broken and superimposed in reddish sandy siltstone.
-2 HH and JH	150 × 30	1 (7–14)	8	A clutch of aggregated eggs in sandy gravelstone, lower part. Diameters of egg shells are variable depending on the degree of erosion.
-3	58 × 45	1 (10–14)	6	Ditto
-4	43 × 35	1 (10–12)	7	Ditto
-5	45 × 40	1 (11–12)	5	A clutch of aggregated eggs in fine sandstone
-6	25	1 (10–11)	2	A pair of 2 eggs in slightly gravelly sandstone, and uppermost part. One egg comprises eroded top and bottom.
4-1 JH	130 × 30	1 (8–11)	8	A clutch of 3 and 5 aggregated eggs in gravelly sandstone with egg shell fragments. 3 eggs in a nest of 75 × 32 cm ² , 5 in a nest of 38 × 35 cm ² .
-2	45 × 18	1 (4.5–10)	3	1 egg at the bottom and 1 egg with superimposed shell fragments in gravelly sandstone
-3	120 × 25	1 (10–13)	4	2 pairs of eggs that are distributed about 50 cm apart each other in gravelly sandstone.
-4	33 × 15	1 (10–14)	2	Largely circled eggshell and a mould of smaller egg in Gzg
-5	31 × 9	1 (3–9)	4	Flattened and smooth surface without ornaments
-6	80 × 57	1 (11)	8	A clutch in gravelly sandstone. 9 eggs excavated; 8 eggs found on the rock surface.
5-1 SH	-	1 (11)	1	In gravelly siltstone with shell fragments
-2	110 × 50	1 (9–13)	9	A clutch of 6 aggregated eggs and top parts of 3 eggs in gravelly sandstone
-3	45 × 15	1 (9–12)	4	A clutch in gravelly sandstone. The top part of egg shells is broken. Some are filled with large breccia, gravel and sand.
-4	130 × 15	1 (6.7–11)	7	Pairs of 3 and 4 in gravelly sandstone, slightly flattened
6-1 H	55 × 22	1 (11–12)	3	Eggs about 7–26 cm apart each other in gravelly sandstone
-2	-	1 (12)	1	In gravelly sandstone, apart about 150 cm from 2 eggs
-3	25	1 (6.5–12)	2	Paired in gravelly sandstone. Top part of smaller egg shell.
-4	180 × 80	1 (10–13)	16	Nests: 9 eggs in 80 × 48 cm ² , 5 eggs in 41 × 21 cm ² , and 2 eggs in 25 × 21 cm ² apart 34 to 45 cm one another
-5	37 × 20	1 (10.5–11)	3	Aggregated in a nest of gravelly sandstone
-6	150 × 60	1 (8.5–11)	7	2 eggs in 36 × 11 cm ² -sized nest, 4 eggs in a nest of 65 × 50 cm ² in gravelly sandstone
-7	95 × 25	1 (9–13)	8	4 eggs in a nest of 45 × 25 cm ² , 3 eggs in 48 × 20 cm ² , and 1 egg in gravelly sandstone
-8	31 × 22	1 (6–11.5)	5	Eggs aggregated in a nest in gravelly sandstone with egg shell fragments
-9	32 × 11	1 (7–11)	4	Linearly aggregated 3 eggs in gravelly sandstone. 1 egg shell is superimposed with shell fragments at the top. One egg occurs about 70 cm apart from 3 eggs.
-10	22 × 11	1 (10.5–11)	2	Eggs with some shell fragments in gravelly sandstone
8-1 G	-	1 (10)	1	Half-circled egg shell in gravelly sandy siltstone
-2	27 × 50	2 (9)	2	Type 2 eggs with very thick (5 mm) shells in siltstone with fragments
-3	35 × 10	2 (-)	3	A clutch of broken egg shells in reddish sandstone beneath gravelstone layer
-4	34 × 40	2 (8)	12	A clutch in reddish sandstone, excavated
9-1 D	52 × 33	1 (10–12)	6	Bottom parts of a clutch in reddish gravelly sandstone of cavity ceiling
-2	110 × 40	1 (11–13)	9	Pairs of 2, 2, and 3 egg shells in gravelly sandstone
-3	101 × 21	1 (8–11.5)	8	Pairs of 2, 4, and 2 egg shells in gravelly sandstone
-4	128 × 23	1 (9–12)	5	Pairs of 3 and 2 eggs in gravelly sandstone 64 cm apart

channel/splay deposits and floodplain fines in the distal part. Alluvial fans mainly ensued from the eastern basin margin and prograded westward, whereas braided streams flowed southward along the western basin margin. Deposition generally occurred in arid to semi-arid climatic conditions.

More than 140 dinosaur eggs occur in either channel-fill conglomerate or massive gravelly siltstone. Eggs commonly retain oval shape, stuffed with the substrate of gravelly siltstone to silty conglomerate. Egg-bearing beds commonly comprise sandy siltstone of floodsheet and trough cross-stratified gravelly sandstone of 3D dunes. Dinosaur eggs were partially reseeded during flash floods from the original nests in alluvial braided streams. This study indicates the importance of sedimentologic analysis for the comprehension of fossil preservation process and guides exploration for dinosaur remains in future excavations.

Acknowledgements

This work was supported by grants to Chough by the Korea Research Foundation (no. R14-2003-017-01000-0, 2003 and no. KRF-2006-312-C00690) and the BK21 Project. We are grateful to Drs. C. W. Rhee, W. H. Ryang and Y. -N. Lee for their helpful

discussions in the field. Thanks are extended to Messrs. Y. J. Shinn and J. Woo for their assistance in the field and laboratory. We would like to express our sincere thanks for the journal reviewers, David Varricchio and an anonymous reviewer, for their critical and constructive comments. S. B. Kim acknowledges the Korea Polar Research Institute for financial support (PE05001).

References

- Allen, J.R.L., 1973. Phase differences between bed configurations and flow in natural environments, and their geological relevance. *Sedimentology* 20, 323–329.
- Allen, J.R.L., 1983. Studies in fluvial sedimentation: bars, bar-complexes and sandstone sheets (low-sinuosity braided streams) in the Brownstones (L. Devonian), Welsh Borders. *Sedimentary Geology* 33, 237–293.
- Arguden, A.T., Rodolfo, K.S., 1986. Sedimentary facies and tectonic implications of lower Mesozoic alluvial-fan conglomerates of the Newark Basin, northeastern United States. *Sedimentary Geology* 51, 97–118.
- Ashmore, P., 1993. Anabranch confluence kinetics and sedimentation processes in gravel-braided streams. In: Best, J.L., Bristow, C.S. (Eds.), *Braided Rivers*. Geological Society London, Special Publications 75, 129–146.
- Bennett, S.J., Bridge, J.S., 1995. An experimental study of flow, bedload transport and bed topography under conditions of erosion and deposition and comparison with theoretical models. *Sedimentology* 42, 117–146.
- Blair, T.C., 1987. Sedimentary processes, vertical stratification sequences, and geomorphology of the Roaring River Alluvial Fan, Rocky Mountain National Park, Colorado. *Journal of Sedimentary Petrology* 57, 1–18.

- Blair, T.C., 1999a. Sedimentology of the debris-flow-dominated Warn Spring Canyon alluvial fan, Death Valley, California. *Sedimentology* 46, 941–965.
- Blair, T.C., 1999b. Sedimentary processes and facies of the waterlaid Anvil Spring Canyon alluvial fan, Death Valley, California. *Sedimentology* 46, 913–940.
- Blair, T.C., 2000. Sedimentology and progressive tectonic unconformities of the sheetflood-dominated Hell's Gate alluvial fan, Death Valley, California. *Sedimentary Geology* 132, 233–262.
- Blair, T.C., McPherson, J.G., 1994. Alluvial fans and their natural distinction from rivers based on morphology, hydraulic processes, sedimentary processes, and facies assemblages. *Journal of Sedimentary Research* 64B, 450–489.
- Boering, M., North, C., 1993a. Dryland alluvial fan deposits: controls on sheetflood development. In: 5th International Conference on Fluvial Sedimentology, Abstracts, Queensland, pp. 14.
- Boering, M., North, C., 1993b. Sedimentology of dryland sheetflood deposits: a quantitative approach. In: 5th International Conference on Fluvial Sedimentology, Abstracts, Queensland, pp. 15.
- Boothroyd, J.C., Ashley, G.M., 1975. Process, bar morphology and sedimentary structures on braided outwash fans, North-eastern Gulf of Alaska. In: Jopling, A.V., McDonald, B.C. (Eds.), *Glaciofluvial and Glaciolacustrine Sedimentation*. Society of Economic Palaeontologist and Mineralogists, Special Publication 23, 193–222.
- Bridge, J.S., 1984. Large-scale facies sequences in alluvial overbank environments. *Journal of Sedimentary Petrology* 54, 583–588.
- Bridge, J., 1993. Description and interpretation of fluvial deposits: a critical perspective. *Sedimentology* 40, 801–810.
- Bridge, J.S., Best, J.L., 1997. Preservation of planar laminae arising from low-relief bed waves migrating over aggrading plane beds: comparison of experimental data with theory. *Sedimentology* 44, 253–262.
- Bristow, C.S., Skelly, R.L., Ethridge, F.G., 1999. Crevasse splays from the rapidly aggrading, sand-bed, braided Niobrara River, Nebraska: effect of base-level rise. *Sedimentology* 46, 1029–1047.
- Bromley, M.H., 1991. Variations in fluvial style as revealed by architectural elements, Kayenta Formation, Mesa Creek, Colorado, USA: evidence for both ephemeral and perennial fluvial processes. Concepts in Sedimentology and Palaeontology. In: Miall, A.D., Tyler, N. (Eds.), *The Three-dimensional Facies Architecture of Terrigenous Clastic Sediments and Its Implication for Hydrocarbon Discovery and Recovery*. Society of Economic Palaeontologist and Mineralogists vol. 3, 99–102. Tulsa, OK.
- Choe, M.Y., Jo, H.R., Lee, J.L., Hur, S.D., Jeong, K.S., 2001. Investigations on the Geology and Subsurface Remains in the Abandoned Tidal Flats (Daebu Island Area) of Sihwa Lake. Ansan city, 101 pp. (in Korean).
- Choi, D.K., 1985. Spores and pollen from the Gyeongsang Supergroup, southeastern Korea and their chronologic and palaeoecologic implications. *Journal of the Palaeontological Society of Korea* 1, 33–50.
- Chough, S.K., Kim, S.B., Chun, S.S., 1996. Sandstone/chert and laminated chert/black shale couples, Cretaceous Uhangri Formation (southwest Korea): depositional events in alkaline lake environments. *Sedimentary Geology* 104, 227–242.
- Chough, S.K., Kwon, S.-T., Ree, J.-H., Choi, D.K., 2000. Tectonic and sedimentary evolution of the Korean Peninsula: a review and new view. *Earth-Science Reviews* 52, 175–235.
- Chun, S.S., Chough, S.K., 1992. Tectonic history of Cretaceous sedimentary basins in the southwestern Korean Peninsula and Yellow Sea. In: Chough, S.K. (Ed.), *Sedimentary Basins in the Korean Peninsula and Adjacent Seas*. Korean Sedimentologists Research Group, Special Publications, 60–76. Harnlimwon Publishers, Seoul.
- Cousin, R., Breton, G., Fournier, R., Watté, J.P., 1994. Dinosaur egg laying and nesting in France. In: Carpenter, K., Hirsch, K.F., Horner, J.R. (Eds.), *Dinosaur Eggs and Babies*. Cambridge University Press, Cambridge, pp. 56–74.
- Crowell, J.C., 1975. The San Gabriel Fault and Ridge Basin, southern California. In: Crowell, J.C. (Ed.), *San Andreas Fault in Southern California*. California Division of Mines and Geology, Special Report 18, 208–219.
- Crowell, J.C., 1982. The Violin Breccia, Ridge Basin, southern California. In: Crowell, J.C., Link, M.H. (Eds.), *Geologic History of Ridge Basin, Southern California*. Society of Economic Palaeontologist and Mineralogists, Pacific Section, 89–98. Field Guide Book.
- Crowley, K.D., 1983. Large-scale bed configurations (macroforms), Platte River Basin, Colorado and Nebraska: primary structures and formative processes. *The Geological Society of America Bulletin* 94, 117–133.
- Davies, T.R.H., 1986. Large debris flows: a macro-viscous phenomenon. *Acta Mechanica* 63, 161–178.
- Davies, T.R.H., 1990. Debris flow surges—experimental simulation. *Journal of Hydrology (New Zealand)* 29, 18–46.
- Deluca, J.L., Eriksson, K.A., 1989. Controls on synchronous ephemeral and perennial-river sedimentation in the middle sandstone member of the Triassic Chinle Formation, northeastern New Mexico, USA. *Sedimentary Geology* 61, 155–175.
- Erben, H.K., Hoefs, J., Wedepohl, K.H., 1979. Paleobiological and isotopic studies of eggshells from a declining dinosaur species. *Paleobiology* 5, 380–414.
- Friend, P.F., 1966. Clay fractions and colours of some Devonian red beds in the Catskill Mountains, U.S.A. *Journal of the Geological Society, London* 122, 273–292.
- Frostick, L.E., Reid, I., 1990. Structural control of sedimentation patterns and implication for the economic potential of the East African Rift basins. *Journal African Earth Sciences* 10, 307–318.
- Gawthorpe, R.L., Colella, A., 1990. Tectonic controls on coarse-grained delta depositional systems in rift basins. In: Colella, A., Prior, D.B. (Eds.), *Coarse-Grained Deltas*. International Association of Sedimentologists, Special Publications 10, 113–128.
- Gloppen, T.G., Steel, R.J., 1981. The deposits, internal structure and geometry in six alluvial fan-fan delta bodies (Devonian–Norway)—a study in the significance of bedding sequence. In: Ethridge, F.G., Flores, R.M. (Eds.), *Recent and Ancient Nonmarine Depositional Environments: models for Exploration*. Society of Economic Palaeontologist and Mineralogists, Special Publication 31, 49–69.
- Goedhart, M.L., Smith, N.D., 1998. Braided stream aggradation on an alluvial fan margin: Emerald Lake fan, British Columbia. *Canadian Journal of Earth Sciences* 35, 534–545.
- Gómez-Villar, A., García-Ruiz, J.M., 2000. Surface sediment characteristics and present dynamics in alluvial fans of the central Spanish Pyrenees. *Geomorphology* 34, 127–144.
- Harms, J.C., Southard, J.B., Spearing, D.R., Walker, R.G., 1982. Structure and Sequences in Clastic Rocks. Society of Economic Palaeontologist and Mineralogists, Short Course No. 9, Calgary, 161 pp.
- Harvey, A., 1984. Debris flows and fluvial deposits in Spanish Quaternary alluvial fans: implications for fan morphology. In: Koster, E.H., Steel, R.J. (Eds.), *Sedimentology of Gravels and Conglomerates*. Canadian Society of Petroleum Geologists, Memoir 10, 123–132.
- Heinz, J., Aigner, T., 2003. Hierarchical dynamic stratigraphy in various Quaternary gravel deposits, Rhine glacier area (SW Germany): implications for hydrostratigraphy. *International Journal of Earth Sciences* 92, 923–938.
- Hirsch, K.F., 1994. Upper Jurassic eggshells from the Western Interior of North America. In: Carpenter, K., Hirsch, K.F., Horner, J.R. (Eds.), *Dinosaur Eggs and Babies*. Cambridge University Press, Cambridge, pp. 137–150.
- Hogg, S.E., 1982. Sheetfloods, sheetwash, sheetflow, or ...? *Earth-Science Reviews* 18, 59–76.
- Hooke, 1967. Processes on arid-region alluvial fans. *Journal of Geology* 75, 438–460.
- Hubert, J.F., Forlenza, M.F., 1988. Sedimentology of braided-river deposits in Upper Triassic Wolfville redbeds, southern shore of Cobequid Bay, Nova Scotia, Canada. In: Manspeizer, W. (Ed.), *Triassic–Jurassic Rifting: Continental Breakup and the Origin of the Atlantic Ocean and Passive Margins*. Development in Geotectonics, vol. 22. Elsevier, Amsterdam, pp. 231–247.
- Huh, M., Hwang, K.G., Paik, I.S., Chung, C.H., Kim, B.S., 2003. Dinosaur tracks from the Cretaceous of South Korea: Distribution, occurrences and palaeobiological significance. *The Island Arc* 12, 132–144.
- Hwasung City, 2005. Report on the Preservation and Characteristics of the Dinosaur Egg Fossil Localities in Hwasung City, Gyeonggi-do. 172 pp. (in Korean).
- Iatzoura, A., Cojan, I., Renard, M., 1991. Géochimie des coquilles d'oeufs de dinosaures: essai de reconstitution paléoenvironnementale (Maastrichtien, bassin d'Aix-en-Provence, France). *Comptes Rendus des Séances de l'Académie des Sciences, Paris* 312, 1343–1349.
- Jo, H.R., 2003. Depositional environments, architecture, and controls of Early Cretaceous non-marine successions in the northwestern part of Kyongsang Basin, Korea. *Sedimentary Geology* 161, 269–294.
- Jo, H.R., Chough, S.K., 2001. Architectural analysis of fluvial sequences in the northwestern part of Kyongsang Basin (Early Cretaceous), SE Korea. *Sedimentary Geology* 144, 307–334.
- Jo, H.R., Rhee, C.W., Chough, S.K., 1997. Distinctive characteristics of a streamflow-dominated alluvial fan deposits: Sanghori area, Kyongsang Basin (Early Cretaceous), southeastern Korea. *Sedimentary Geology* 110, 51–79.
- Jorgensen, P.J., Fielding, C.R., 1996. Facies architecture of alluvial floodbasin deposits: three-dimensional data from the Upper Triassic Callide Coal Measures of east-central Queensland, Australia. *Sedimentology* 43, 479–495.
- Karpeta, W.P., 1993. Sedimentology and gravel bar morphology in an Archean braided river sequence: the Witpan Conglomerate Member (Witwatersrand Supergroup) in the Welkom Goldfield, South Africa. In: Best, J.L., Bristow, C.S. (Eds.), *Braided Rivers*. Geological Society London, Special Publications 75, 369–388.
- Khadikar, A.S., 1999. Trough cross-bedded conglomerate facies. *Sedimentary Geology* 128, 39–49.
- Kim, B.C., Lowe, D.R., 2004. Depositional processes of the gravelly debris flow deposits, South Dolomite alluvial fan, Owens Valley, California. *Geosciences Journal* 8, 153–170.
- Kim, S.B., Chough, S.K., Chun, S.S., 1995. Bouldery deposits in the lowermost part of the Cretaceous Kyokpori Formation, SW Korea: cohesionless debris flows and debris falls on a steep-gradient delta slope. *Sedimentary Geology* 98, 97–119.
- Kim, S.B., Chun, S.S., Chough, S.K., 1997. Discussion on structural development and stratigraphy of the Kyokpo pull-apart basin, South Korea and tectonic implications for inverted extensional basins. *Journal of the Geological Society, London* 154, 369–372.
- Kim, S.B., Chough, S.K., Chun, S.S., 2003. Tectonic controls on spatio-temporal development of depositional systems and generation of fining-upward basin fills in a strike-slip setting: Kyokpori Formation (Cretaceous), south-west Korea. *Sedimentology* 50, 639–666.
- Kochel, R.C., 1990. Humid fans of the Appalachian Mountains. In: Rachocki, A.H., Churc, M. (Eds.), *Alluvial Fans: a Field Approach*. Wiley, Chichester, pp. 109–129.
- Lambiase, J.J., Bosworth, W.P., 1995. Structural development and stratigraphy of the Kyokpo Pull-Apart Basin, South Korea and tectonic implications for inverted extensional basins. In: Buchanan, J.G., Buchanan, P.G. (Eds.), *Basin Inversion*. Geological Society London, Special Publications 31, 457–471.
- Leddy, J.O., Ashworth, P.J., Best, J.L., 1993. Mechanisms of anabranch avulsion within gravel-bed braided rivers: observations from a scaled physical model. In: Best, J.L., Bristow, C.S. (Eds.), *Braided Rivers*. Geological Society London, Special Publications 75, 119–127.
- Lee, D.-W., 1999. Strike-slip fault tectonics and basin formation during the Cretaceous in the Korean Peninsula. *The Island Arc* 8, 218–231.
- Lee, B.-J., Lee, S.R., Cho, D.-L., 1999a. Geological Map and Explanatory Text of Dae-budo Sheet (1:50000). Korea Institute Geology Mining and Materials, Taejon, 33

- pp. (in Korean).
- Lee, B.-J., Kim, Y.B., Lee, S.R., Kim, J.C., Kang, P.-C., Choi, H.-I., Jin, M.-S., 1999b. Geological Map and Explanatory Note of Seoul-Namchonjeom Sheet (1: 250000). Korea Ministry of Science and Technology, Taejon, 64 pp. (in Korean).
- Lee, Y.-N., Jeong, K.S., Chan, S.K., Choi, M.Y., Choi, J.I., 2000. The preliminary research on the dinosaur eggs and nests found in the reclaimed area south to the Sihwa Lake, Gyeonggi Province, Korea. *Journal of the Palaeontological Society of Korea* 16, 27–36.
- Lee, Y.-N., Yu, K.-M., Wood, C.B., 2001. A review of vertebrate faunas from the Gyeongsang Supergroup (Cretaceous) in South Korea. *Palaeogeography Palaeoclimatology Palaeoecology* 165, 357–373.
- Leeder, M.R., 1988. Development of alluvial fans and fan deltas in neotectonic extensional settings: implications for the interpretation of basin fills. In: Nemecek, W., Steel, R.J. (Eds.), *Fan Deltas: Sedimentology and Tectonic Settings*. Blackie, Glasgow, pp. 173–185.
- Leeder, M.R., 1995. Continental rifts and proto-oceanic rift troughs. In: Busby, C.J., Ingersoll, R.V. (Eds.), *Tectonics of Sedimentary Basins*. Blackwell Scientific Publications, Oxford, pp. 119–148.
- Luttrell, P.R., 1993. Basinwide sedimentation and the continuum of palaeoflow in an ancient river system: Kayenta Formation (Lower Jurassic), central portion Colorado Plateau. *Sedimentary Geology* 85, 411–434.
- Mack, G.H., Rasmussen, K.R., 1984. Alluvial-fan sedimentation of the Cutler Formation (Permo-Pennsylvanian) near Gateway, Colorado. *The Geological Society of America, Bulletin* 95, 109–116.
- Major, J.R., 1997. Depositional processes in large-scale debris-flow experiments. *Journal of Geology* 105, 345–366.
- Marshall, J.D., 2000. Sedimentology of a Devonian fault-bounded braidplain and lacustrine fill in the lower part of the Skrinkle Sandstones, Dyfed, Wales. *Sedimentology* 47, 325–342.
- Miall, A.D., 1977. A review of the braided river depositional environments. *Earth-Science Reviews* 13, 1–62.
- Miall, A.D., 1985. Architectural-element analysis: a new method of facies analysis applied to fluvial deposits. *Earth-Science Reviews* 22, 261–308.
- Miall, A.D., 1996. *The Geology of Fluvial Deposits*. Springer, Berlin, 582 pp.
- Mjøs, R., Walderhaug, O., Prestholm, E., 1993. Crevasse splay sandstone geometries in the Middle Jurassic Ravenscar Group of Yorkshire, UK. In: Marzo, M., Puigdefabregas, C. (Eds.), *Alluvial Sedimentation*. International Association of Sedimentologists, Special Publications 17, 167–184.
- Mulder, T., Alexander, J., 2001. The physical character of subaqueous sedimentary density flows and their deposits. *Sedimentology* 48, 269–300.
- Nemecek, W., Steel, R.J., 1984. Alluvial and coastal conglomerates: their significant features and some comments on gravelly mass-flow deposits. In: Koster, E.H., Steel, R.J. (Eds.), *Sedimentology of Gravels and Conglomerates*. Canadian Society of Petroleum Geologists, Memoir 10, 1–31.
- Nemecek, W., Postma, G., 1993. Quaternary alluvial fans in southwestern Crete: sedimentation processes and geomorphic evolution. In: Marzo, M., Puigdefabregas, C. (Eds.), *Alluvial Sedimentation*. International Association of Sedimentologists, Special Publications 17, 235–276.
- Nilsen, 1982. Alluvial fan deposits. In: Scholle, P.A., Spearing, D. (Eds.), *Sandstone Depositional Environments*. American Association of Petroleum Geologists, Memoir 31, 50–86.
- Nilsen, T.H., McLaughlin, R.J., 1985. Comparison of tectonic framework and depositional patterns of the Hornelen strike-slip basin of Norway and the Ridge and Little Sulphur Creek strike-slip basin of California. In: Biddle, K.T., Christie-Blick, N. (Eds.), *Strike-Slip Deformation, Basin Formation, and Sedimentation*. Society of Economic Palaeontologist and Mineralogists, Special Publication 37, 79–104.
- Paik, I.S., Chun, J.H., 1993. Laminar calcretes, calcrete pisoids and ooids, and rhizoliths from the Gyeongsang Supergroup, Korea. *Journal of Geological Society of Korea* 29, 108–117.
- Paik, I.S., Kim, H.J., 2003. Palustrine calcretes of the Cretaceous Gyeongsang Supergroup, Korea: variation and palaeoenvironmental implications. *The Island Arc* 12, 110–124.
- Paik, I.S., Lee, Y.I., 1998. Desiccation cracks in vertic palaeosols of the Cretaceous Hasandong Formation, Korea: genesis and palaeoenvironmental implications. *Sedimentary Geology* 119, 161–179.
- Paik, I.S., Kim, H.J., Lee, Y.I., 2001a. Dinosaur track-bearing deposits in the Cretaceous Jindong Formation, Korea: occurrence, palaeoenvironments and preservation. *Cretaceous Research* 22, 79–92.
- Paik, I.S., Kim, H.J., Park, K.H., Song, Y.S., Lee, Y.I., Hwang, J.Y., Huh, M., 2001b. Palaeoenvironments and taphonomic preservation of dinosaur bone-bearing deposits in the Lower Cretaceous Hasandong Formation, Korea. *Cretaceous Research* 22, 627–642.
- Paik, I.S., Huh, M., Kim, H.J., 2004. Dinosaur egg-bearing deposits (Upper Cretaceous) of Boseong, Korea: occurrence, palaeoenvironments, taphonomy, and preservation. *Palaeogeography Palaeoclimatology, Palaeoecology* 205, 155–168.
- Paola, C., Wiele, S.M., Reinhart, M.A., 1989. Upper-regime parallel lamination as the result of turbulent sediment transport and low-amplitude bed forms. *Sedimentology* 36, 47–59.
- Park, N.Y., Kim, J.H., 1972. Geological Map and Explanatory Text of Namyang Area (1: 50000). Korea Institute of Geology Mining and Materials, Teajon, 13 pp. (in Korean with English abstract).
- Park, S.D., 2000. Analysis of Sedimentary Basin in the Sihwa Area, Hwasunggun and Tando area, Ansanshi, Kungki Province, Korea. Unpubl. MSc thesis, Chungnam National University, 119 pp. (in Korean with English abstract).
- Park, S.-D., Chung, G.-S., Jeong, J.-G., Kim, W.-S., Lee, D.-W., Song, M.-Y., 2000. Structure and physical property of the crust of mid-west Korea: analysis of sedimentary basins in the Sihwa and Tando areas, Gyeonggi Province, Korea. *Journal of Korean Earth Science Society* 21, 563–582 (in Korean with English abstract).
- Retallack, G.J., 1997. *A Colour Guide to Palaeosols*. Wiley, Chichester, 175 pp.
- Rhee, C.W., Chough, S.K., 1993a. The Cretaceous Pyonghae Basin, Southeast Korea - Sequential development of crevasse splay and avulsion in a terminal alluvial-fan. *Sedimentary Geology* 83, 37–52.
- Rhee, C.W., Chough, S.K., 1993b. The Cretaceous Pyonghae sequence, Southeast Korea: terminal fan facies. *Palaeogeography Palaeoclimatology, Palaeoecology* 105, 139–156.
- Rhee, C.W., Ryang, W.H., Chough, S.K., 1993. Contrasting development patterns of crevasse channel deposits in Cretaceous alluvial successions, Korea. *Sedimentary Geology* 85, 401–410.
- Ritter, J.B., Miller, J.R., Howes, E.S.D., Nadon, G., Grubb, M.D., Hoover, K.A., Olsen, T., Reneau, S.L., Sack, D., Summa, C.L., Taylor, I., Touyinhthiphonexay, K.C.N., Yodis, E.G., Schneider, N.P., Ritter, D.F., Wells, S.G., 1993. Quaternary evolution of Cedar Creek alluvial fan, Montana. *Geomorphology* 8, 287–304.
- Rust, B.R., 1978. Depositional models for braided alluvium. In: Miall, A.D. (Ed.), *Fluvial Sedimentology*. Canadian Society of Petroleum Geologists, Memoir 5, 187–198.
- Sadler, S.P., Kelly, S.B., 1993. Fluvial processes and cyclicity in terminal fan deposits - An example from the Late Devonian of Southwest Ireland. *Sedimentary Geology* 85, 375–386.
- Sanderson, D.J., Marchini, W.R.D., 1984. Transpression. *Journal of Structural Geology* 6, 449–458.
- Sanz, J.L., Moratalla, J.J., Díaz-Molina, M., López-Martínez, N., Kälin, O., Vianey-Liaud, M., 1995. Dinosaur nests at the sea shore. *Nature* 376, 731–732.
- Schubert, C., 1980. Late-Cenozoic pull-apart basins, Bocono fault zone, Venezuelan Andes. *Journal of Structural Geology* 2, 463–468.
- Sharp, R.P., Nobles, L.H., 1953. Mudflows in 1941 at Wrightwood, southern California. *The Geological Society of America, Bulletin* 64, 547–560.
- Simons, D.B., Richardson, E.V., 1966. Resistance to Flow in Alluvial Channels. U.S. Geological Survey, Professional Paper 422, 61.
- Sohn, Y.K., Kim, S.B., Hwang, I.G., Bahk, J.J., Choe, M.Y., Chough, S.K., 1997. Characteristics and depositional processes of large-scale gravelly Gilbert-type foresets in the Miocene Doumsan fan-delta, Pohang Basin, SE Korea. *Journal of Sedimentary Research* 67, 130–141.
- Sohn, Y.K., Rhee, C.W., Kim, B.C., 1999. Debris flows and hyperconcentrated flood-flow deposits in an alluvial fan, northwestern part of the Cretaceous Yongdong Basin, central Korea. *Journal of Geology* 107, 111–132.
- Stear, W.M., 1983. Morphological characteristics of ephemeral stream channel and overbank splay sandstone bodies in the Permian Lower Beaufort Group, Karoo Basin, South Africa. In: Collinson, J.D., Lewin, J. (Eds.), *Modern and Ancient Fluvial Systems*. International Association of Sedimentologists, Special Publications 6, 405–420.
- Stear, W.M., 1985. Comparison of the bedform distribution and dynamics of modern and ancient sandy ephemeral flood deposits in the southwestern Karoo region, South Africa. *Sedimentary Geology* 45, 209–230.
- Steel, R.J., 1974. New Red Sandstone floodplain and piedmont sedimentation in the Hebridian Province, Scotland. *Journal of Sedimentary Petrology* 44, 336–357.
- Steel, R.J., Gloppen, T.G., 1980. Late Caledonian (Devonian) basin formation, western Norway: signs of strike-slip tectonics during infilling. In: Reading, H.G., Balance, P.F. (Eds.), *Sedimentation in Oblique-Slip Mobile Zones*. International Association of Sedimentologists, Special Publications 4, 79–104.
- Steel, R.J., 1988. Coarsening-upward and skewed fan bodies: symptoms of strike-slip and transfer fault movement in sedimentary basins. In: Nemecek, W., Steel, R.J. (Eds.), *Fan Deltas: Sedimentology and Tectonic Settings*. Blackie, Glasgow, pp. 75–83.
- Tunbridge, I.P., 1981. Sandy high-energy flood sedimentation—some criteria for recognition, with an example from the Devonian of SW England. *Sedimentary Geology* 28, 79–95.
- Turner, P., 1980. *Continental Red Beds*. Elsevier, Amsterdam, 562 pp.
- van der Straaten, H.C., 1990. Stacked Gilbert-type deltas in the marine pull-apart basin of Abaran, late Serravalian-early Tortonian, southeastern Spain. In: Colella, A., Prior, D.B. (Eds.), *Coarse-Grained Deltas*. International Association of Sedimentologists, Special Publications 10, 199–222.
- Wells, S.G., Harvey, A.M., 1987. Sedimentologic and geomorphic variations in storm-generated alluvial fans, Howgill fells, northwest England. *The Geological Society of America, Bulletin* 98, 182–198.
- Whiting, P.J., Dietrich, W.E., Leopold, L.B., 1988. Bedload sheets in heterogeneous sediment. *Geology* 16, 105–108.
- Woo, K.S., Lee, K.C., Paik, K.H., 1991. Cretaceous lacustrine radial ooids in the Kyongsang Basin, Korea: palaeoclimatic implications. *Journal of Geological Society of Korea* 27, 171–176.
- Zhao, Z.K., 1979. The advancement of research on the dinosaurian eggs in China. In: IVPP, N.G.P.I. (Ed.), *Mesozoic and Cenozoic Redbeds in Southern China*. Beijing Science Press, Beijing, pp. 330–340.
- Zhao, Z.K., Ding, S.R., 1976. Discovery of the dinosaurian eggshells from Alaxa, Ningxia and its stratigraphical significance. *Vertebrata Palasiatica* 14, 42–51.
- Zhao, Z.K., Li, Z.C., 1988. A new structural type of the dinosaur eggs from Anlu County, Hubei Province. *Vertebrata Palasiatica* 26, 107–115.